FOUNDATION FOR RESEARCH AND TECHNOLOGY - HELLAS
INSTITUTE OF MOLECULAR BIOLOGY AND BIOTECHNOLOGY

UNIVERSITY OF CRETE

DNA damage-induced inflammation in neurodegeneration

Electra Nenedaki

Master thesis

Graduate student of "Molecular Biology and Biomedicine" program, University of Crete, IMBB-Forth, 2017-2019

Advisor: Professor George Garinis, laboratory of Genome (In)stability and Mammalian Physiology (Institute of Molecular Biology and Biotechnology, IMBB-FORTH)

Supervisor: Post- doctoral researcher Katerina Gkirtzimanaki

ABSTRACT

Microglia cells are the brain resident macrophages. Microglia promote phagocytic clearance, provide trophic support to ensure tissue repair, protect neurons and maintain brain homeostasis. In this study we used a monocyte/macrophage-specific Ercc1-/- mouse (Cx3cr1-Cre) to impair DNA repair in tissue resident macrophages. According to our mouse phenotype, cerebellar ataxia- like neuropathology, we focused our research in microglia. The purpose of this study is to examine whether microglia- specific DNA damage accumulation is enough to drive age- related neuropathology. DNA damage accumulation in microglia cells leads to cytoplasmic presence of damaged chromatin fragments. There are indications that chromatin fragments are transported in the cytoplasm through nucleophagy. Cytoplasmic DNA triggers microglia priming in a cell autonomous manner through type I IFN response. Furthermore, these chromatin fragments are secreted to the extracellular space through microglia derived exosomes. Type I IFN signaling in combination with exosomes lead to Purkinje cells apoptosis, effectively promoting neurodegeneration.

ΠΕΡΙΛΗΨΗ

Τα μικρογλοιακα κύτταρα αποτελούν τα ιστικά μακροφάγα του εγκεφάλου. Συμμετέχουν στη διατήρηση της ομοιόστασης του εγκεφάλου καθώς φαγοκυτταρώνουν τοξικά στοιχεία και προστατεύουν τους νευρώνες. Στην παρούσα μελέτη χρησιμοποιήθηκε ένα μοντέλο ποντίκι με απαλοιφή του γονιδίου της Ercc1 στα ιστικά μακροφάγα, οδηγώντας σε προβληματική επιδιόρθωση των γενετικών βλαβών και παρουσίασε κινητικά προβλήματα στην ενήλικη ζωή του, χαρακτηριστικά της παρεγεφαλιδικής αταξίας. Εξαιτίας της νευρολογικής φύσης του φαινοτύπου, η μελέτη επικεντρώθηκε στη μικρογλοία. Σκοπός της εργασίας αυτής είναι να διαλευκανθεί ο ρόλος της συσσώρευσης γενετικών βλαβών στη μικρογλοία, στην εξέλιξη του νευροεκφυλισμού. Η συσσώρευση γενετικών βλαβών οδηγεί στη μεταφορά κατεστραμμένων κομματιών χρωματίνης στο κυτταρόπλασμα, πιθανόν μέσω πυρηνοφαγίας. Η παρουσία του κυτταροπλασματικού DNA ενεργοποιεί προφλεγμονωδώς τα μικρογλοιακά κύτταρα μέσω παραγωγής ιντερφερονών τύπου Ι. Παράλληλα, τα κομμάτια χρωματίνης εκκρίνονται στον εξωκυττάριο χώρο μέσω εξωσωμάτων. Οι ιντερφερόνες τύπου Ι καθώς και τα εξωσώματα γίνονται αντιληπτά από τα Purkinje νευρικά κύτταρα, προκαλώντας τον θάνατο τους και οδηγώντας σταδιακά σε νευροεκφυλισμό.

Table of contents

Chapter I:

Introduction

1.1 DNA damage and DNA repair pathways

The genomes of all organisms are constantly being modified by reactive molecules that are produced endogenously or exogenously. There are various endogenous physiological processes that lead to DNA aberrations in organisms, such as DNA replication, abortive topoisomerase I and topoisomerase II activities, hydrolytic reactions, reactive oxygen compounds by mitochondrial respiration and methylations (Chatterjee et al., 2017). Exogenous DNA damage, on the other hand, occurs when environmental, physical and chemical agents damage the DNA. Examples include UV and ionizing radiation, alkylating agents, crosslinking agents, chemotherapeutic drugs and inflammatory responses. Together, they generate single- or double-strand breaks, intra- or inter-strand DNA crosslinks, or base modifications (figure 1) that could interfere with physiological cellular processes while also contribute to cancer, certain human diseases (including neurodegenerative diseases) and aging (Iyama et al., 2013).

After the DNA is damaged, lesion-specific sensor proteins initiate a DNA damage response (DDR). The DDR is a collection of mechanisms that sense DNA damage, signal its presence and promote subsequent repair (Harper et al., 2007). In fact, DDR is used to provide a time window for DNA repair. DNA damage is repaired by different repair mechanisms depending on the type of lesion, location in the genome and cell cycle phase. The major DNA repair mechanisms are mismatch repair (MMR), base-excision repair (BER), interstrand crosslink (ICL) repair, double-strand break (DSB) repair (including homologous recombination (HR) and nonhomologous end-joining (NHEJ) and nucleotide excision repair (NER) (Morita et al., 2010 ; Chatterjee et al., 2017) (figure 1, Helena et al., 2018).

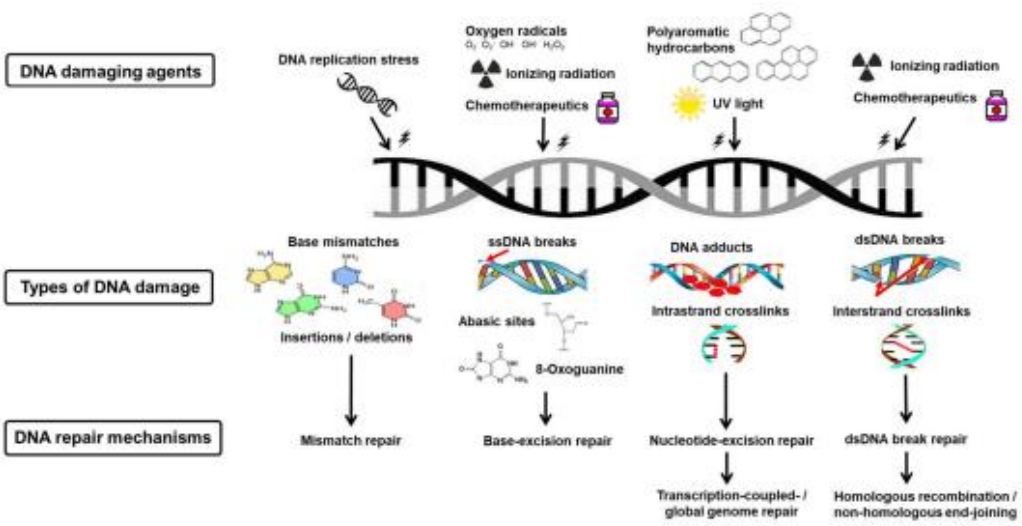

Figure 1: DNA damage and DNA repair pathways.

1.2 DNA repair deficient syndromes

DNA repair defects can cause cancer, inflammation and senescence, main characteristics of aging. The most well-known syndromes are those related to NER deficiency. In humans, inborn mutations in NER genes are associated with syndromes that are both heterogeneous and pleiotropic. Defects in GG-NER give rise to the skin cancer-prone disorder xeroderma pigmentosum-XP (affected proteins: XPA- XPG). Instead, defects in TC-NER(mainly) lead to a heterogeneous group of progeroid disorders that are phenotypically distinct from XP, including the Cockayne syndrome-CS (affected proteins: CSA, CSB, UVSSA, XPB, XPD, XPF and XPG) and Trichothiodystrophy-TTD (affected proteins: XPB, XPD, TTDA) (Marteijn et al., 2014). It is worth to notice that different mutations in the XPB, XPD, XPG genes are linked with a specific clinical outcome, either XP, or XP/CS or TTD (Niedernhofer et al., 2008; Boer et al., 2000). The common feature of these three syndromes is hypersensitivity to UV light, whereas they have different spectrum of clinical symptoms.

XP patients mainly develop basal cell carcinomas, whereas progressive neurologic abnormalities are displayed in a small fraction of these patients. The development of neurologic symptoms depends on the syndrome's stage. This is probably why mutations, in the majority of XP genes, lead to neuronal death. CS patients display skeletal abnormalities and early onset progressive neurodegeneration (Jaarsma et al., 2013). The heterogeneity of Cockayne syndrome-CS is great, as well as CSB ko mice display only mild symptoms, but CSB/XPA double mutant mice suffer from severe growth failure and die before weaning. TTD patients present with the characteristic Sulphur-deficient, dry and sparse hair and nails of TTD, congenital ichthyosis, physical and mental retardation. Consequently, XP, CS and TTD besides otherç, are also related to neurodegeneration (Kamileri et al., 2012). A comparative analysis of neuropathological abnormalities in mouse models for these syndromes suggests the importance of the NER for neuronal integrity and survival. The presence of progressive juvenile or adult onset neurological abnormalities in XP-A patients has provided a strong hint that the NER pathway is important for neuronal function and maintenance.

However, mice models do not fully represent the heterogeneity of patients in NER clinical syndromes. Phenotypic similarities between human and mouse, was mainly observed in double mutants, combining defects in both GG-NER and TC-NER, such as Csb-/- Xpa-/- and $Xpd^{TTD/TTD}$ $Xpa^{-/-}$. Other single mutant animals e.g. Xpc-/-, Csbm/m or Xpa-/- mice result in phenotypically healthy mice with minor pathological symptoms (Niedernhofer et al., 2008). This observation leads to the conclusion that NER factors may involve in other DNA repair pathways and transcription.

1.3 ERCC1 role

The ERCC1-XPF heterodimer is a 5'-3' structure-specific endonuclease that is involved in different DNA repair pathways in mammalian cells. In the ERCC1-XPF heterodimer, ERCC1 is catalytically inactive and instead regulates DNA and protein-protein interactions, while XPF provides the endonuclease activity and contains an inactive helicase-like motif and is involved in DNA binding and additional protein-protein interactions (Faridounnia et al., 2018). ERCC1-XPF cleaves DNA at ds- to ss- junctions, nicking the ds- DNA on the 5' strand 2 nucleotides from the junction ERCCI is implicated in Nucleotide excision repair (NER) (major role), and recruitment of ERCC1-XPF is thought to be mediated by both ERCC1/XPA and XPF/RPA interactions. In addition, ERCC1-XPF has important in double-strand break repair (DSBR) and interstrand crosslink (ICL) repair (Ahmad et al., 2008; Niedernhofer et al., 2004) (figure 2, Vaezi et al., 2011). Studies have shown non-repair related roles for ERCC1 and XPF. ERCC1-XPF complex is involved in telomere maintenance. After knock-down of ERCC1, but not XPF, in

human hepatocellular carcinoma cells, cell cycle delay and multinucleation was observed, suggesting a possible role for ERCC1 protein in mitotic progression.

Only two patients with ERCC1 mutations have been observed. The first patient, 165TOR, has a Gln158Stop mutation inherited from the mother and a Phe231Leu mutation from the father. The clinical diagnosis was cerebro-oculo-facio-skeletal syndrome (COFS), including cerebellar hypoplasia, skeletal defects at birth and severe growth and development delay (Jaspers et al.,2007). The second patient, XP202DC, harbouring a Lys226X nonsense mutation with an IVS6-26G-A splice mutation. The patient displayed progressive neurodegeneration resulting in dementia. Symptoms onset was at age 15 years and died by the age of 37(Gregg et al.,2012).

The knockout mice for Ercc1 (Ercc1 KO) display accelerated aging of multiple organ systems, dystonia, tremors, ataxia and die about 4 weeks of age (Niedernhofer et al., 2006). It was shown that Ercc1 is involved in RNA pol II assembly on promoters (Kamileri et al., 2012). Consistent with this observation, severe developmental failure of Ercc1$^{-/-}$ mice may be the result of perturbed RNA polymerase II transcription initiation. Mice lacking ERCC1 display increased genome instability and chronic expression of inflammatory cytokines, leading to premature aging and early death.

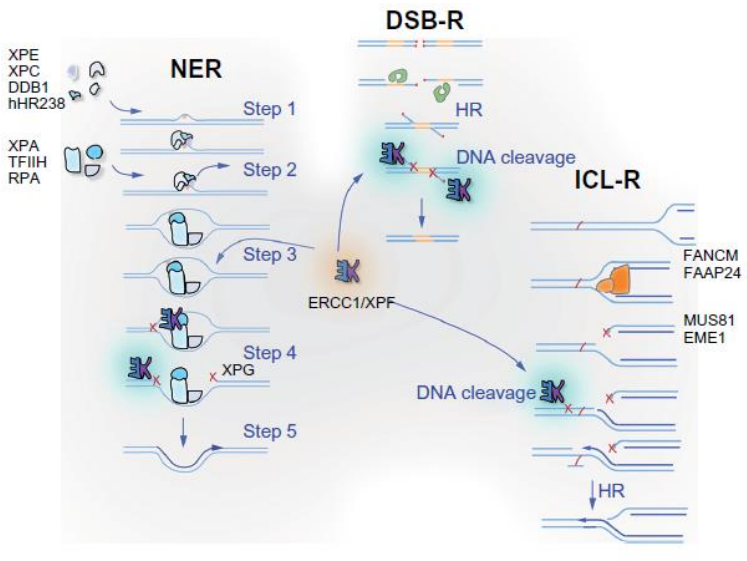

Figure 2: ERCC1-XP is involved in different DNA repair pathways.

1.4 Mouse model

Our lab designed and generated a monocyte/macrophage-specific Ercc1-/- mouse (Cx3cr1-Cre)- progeroid mouse model to impair DNA repair pathways in resident phagocytic populations, such as microglia of the brain (Ercc1 depletion and DNA damage accumulation is specific to Mac1 (CD11b) positive cells). The expression of the fractalkine receptor Cx3CR1 has been identified as a key regulator of macrophage function at sites of inflammation (Zhao et al., 2019; Burgess et al., 2019). Preliminary observations provide evidence that persistent DNA damage triggers microglial activation (ramified morphology) and cerebellar ataxia-like neuropathology in mice with symptoms onset at four months (altered hindlimb clasping behavior, impairment of coordinated movement of legs, tremor and kyphosis).

1.5 Accumulation of DNA damage drives ageing, inflammation and neurodegeneration

Although there is a plethora of repair mechanisms available to the cell for genomic maintenance, DNA damage accumulates with age, primarily caused by an increase in reactive oxygen species and a decrease in DNA repair capacity with age. Accumulation of DNA prevents physiological functions or processes such as DNA replication and transcription and leads to genomic instability (Garinis et al., 2008). DNA damage outcomes are cellular senescence or apoptosis, which in turn leads to compromised tissue homeostasis, most likely through diminished self-renewal or altered tissue structure, organ dysfunction and ageing (Chen et al., 2007). Deficiency in DNA repair pathways, such as NER deficiency, plays a causative role in accelerated ageing as indicated by the NER syndromes displaying progeria (Schumacher et al., 2008).

Main characteristic of ageing is age-related diseases including neurodegeneration, cancer and chronic inflammation. This is consistent with the observation that DNA damage accumulation through NER deficiency results to oxidative stress that drive chronic inflammation, metabolic changes and lipodystrophy (Karakasilioti et al., 2013). Furthermore, there is evidence that DNA repair pathways and other components of the DDR play a role in preventing neuropathology (Maynard et al., 2018). Neurodegeneration is a phenomenon associated with loss of neuronal structure and function. Neurons are vulnerable to DNA damage in due to the low DNA repair capacity of postmitotic brain tissue. Appropriate responses to different type of lesions, like double-stranded breaks or single-stranded breaks are crucial for the normal brain development (Madabhushi et al., 2014). Chronic accumulation of excess oxidative damage and chronic inflammation (sustained activation of microglia-immune defense of the brain) contribute to the development of two main neurodegenerative diseases, Alzheimer's disease (AD) and Parkinson's disease (PD) (Canugovi et al., 2013; Wyss-Coray et al., 2016). For instance, in these diseases, increased levels of DNA lesions and decrease in BER capacity have been observed. Neurotoxicity and neuroprotection are main signatures of inflammation. Under normal conditions, these opposite responses are in balance, but with age, the balance is compromised leading to neurodegenerative diseases (Chen et al., 2016) (figure 3, Chow et al., 2015).

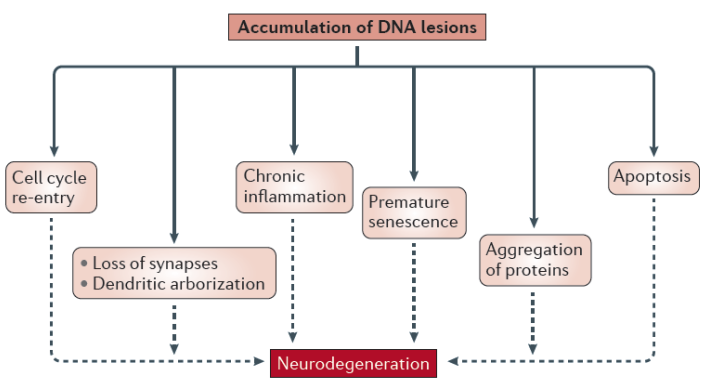

Figure 3: Accumulation of DNA lesions drives ageing, chronic inflammation and neurodegeneration.

1.6 DNA damage response and innate immunity

1.6.1 DNA damage response (DDR)

To counteract the threat of genomic DNA lesions, organisms have evolved a sophisticated network of DNA damage response (DDR) systems. These include events that lead to activation of DNA repair, cell-cycle arrest and tolerance of DNA damage. The principal DDR regulators are two evolutionally conserved kinases, ATM and ATR. Dysregulation of DDR and repair systems can lead to several human disorders that are associated with cancer susceptibility, accelerated aging, and developmental abnormalities. How does it work? Briefly, DNA damage sensors recognize the DNA lesions, transducers are recruited at the site of damage, which, in turn, transmit the damage signals to effectors proteins. This cascade eventually leads to activation of cell cycle checkpoint control and other cellular processes to ensure sufficient DNA repair (Chatzinikolaou et al., 2014).

The DNA damage response (DDR) pathway is composed of different DNA damage sensors: the MRE11–RAD50–NBS1 (MRN) complex and Ku70 that detect DNA double strand breaks (DSBs), the replication protein A (RPA) and the RAD9–RAD1–HUS1 (9-1-1) complex that detects exposed regions of single-stranded DNA (including replication stress), MutS proteins that detect mismatched bases, DNA glycosylases that sense damaged bases and the XPC–RAD23–CETN2 complex that recognizes UV-induced DNA lesions. These sensors recruit the apical kinases ataxia telangiectasia mutated (ATM), ataxia telangiectasia and Rad3-related (ATR), which is bound by ATR-interacting protein (ATRIP) and DNA-PKs. Following this, kinases phosphorylate (P) the histone variant H2AX on Ser139 (known as γH2AX) in the region proximal to the DNA lesion (damage marker). This phosphorylation is required to recruit mediator of DNA damage checkpoint 1 (MDC1) that further sustains and amplifies DDR signaling. Activation of DDR leads to the phosphorylation and stabilization of effectors proteins, such as p53, inducing its nuclear accumulation and upregulation of its target genes. DDR mechanism can cause transient cell cycle arrest followed by repair of DNA damage, cell death by apoptosis and if DNA damage sustains unrepaired, DDR leads to cellular senescence (figure 4, Sulli et al., 2012).

ATM exists as multimeric form, which is dissociated into active monomers upon DNA damage. After double stranded-DNA damage sensing, nuclear ATM is rapidly auto-phosphorylated and mobilizes to the sites of damage. In contrast to ATM and DNA-PKs, which respond primarily to DSBs, ATR is activated by a much wider range of genotoxic stresses that induce the accumulation of ssDNA.

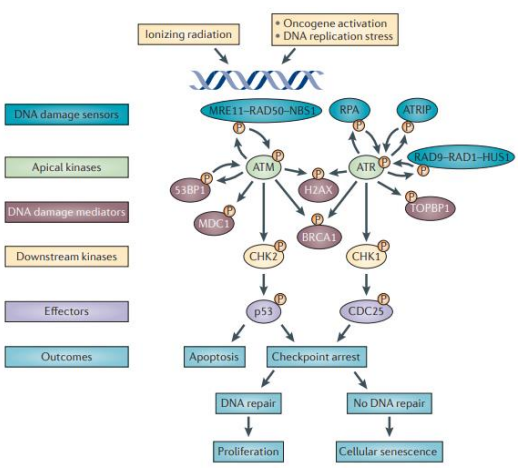

Figure 4: DNA damage response (DDR) pathway.

1.6.2 At the intersection of DNA damage and innate immunity

To protect our-selves against invading pathogens or damaged cells, DNA repair mechanisms and immune defense strategies must be functionally linked and closely coordinated. Innate immune system, primarily, recognizes pathogen-associated molecular patterns -PAMPs or signals derived from damaged macromolecules or dying cells, damage-associated molecular patterns -DAMPs through pattern recognition receptors- PRRs (Stratigi et al., 2016; Tang et al., 2012). There is a plethora of DNA sensors in the cytoplasm, which binds single-stranded or double stranded DNA, inducing an immune response (proinflammatory signals). For instance, DAI (DNA-dependent activator of IFN regulatory factors), DDX41 (DExD/H-box helicase 41), cGAS (cGMP-AMP synthase) and IFI16 (Interferon gamma-inducible protein16) bind cytoplasmic DNA, inducing type I interferon(IFN) response through TBK1(TANK-binding kinase 1) / STING(Stimulator of IFN genes). Furthermore, the innate immune adaptor CARD9 binds DNA activating NF-kB signaling, TLR9, located in the endosome, recognizes single-stranded DNA, in turn, activates IFN or NF-kB signaling through recruitment of MyD88 (Myeloid differentiation marker 88) and RNA polymerase III induces NF-kB activation (figure 5, Nakad et al., 2016).

It is worth to notice that proteins involved in DNA damage response and DNA repair, are present in the cytoplasm as DNA sensors. MRE11/RAD50, Ku70/80, and DNA-PK also bind cytoplasmic dsDNA, in turn, interact with STING pathway, inducing an IRF (IFN regulatory factor) response (figure 5). There is evidence that DNA damage induces IFN signaling. In human cells treated with etoposide, an agent causes double-stranded DNA breaks, is observed expression of IFN-α and IFN-λ genes in a NF-kB- dependent manner (Nakad et al., 2016; Ioannidou et al., 2016). Cells with deficient NEMO (NF-κB essential modulator), lack the ability to induce the IFN genes following DNA damage (Chatzinikolaou et al., 2014). Consequently, there is a functional link between DDR and innate immune signaling, which is strongly related to Nucleotide excision repair syndromes. In fact, the presence of type I IFN immune responses and a DNA damage-driven pro-inflammatory senescence- associated secretory phenotype (SASP) in Cockayne Syndrome (CS) and Trichothiodystrophy (TTD) patients, may contribute to accelerating ageing symptoms (progeroid syndromes) (Kamilerti et al., 2012). Evolutionarily, the link between DNA damage and immune defense may attribute to the need for viral DNA to cause DNA lesions during integration to genomic DNA.

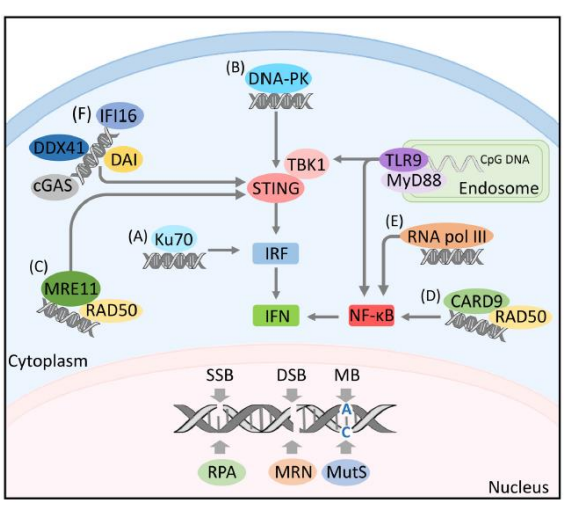

Figure 5: DNA sensors and immune signaling.

1.7 Cytoplasmic DNA triggers type I IFN response.

1.7.1 Type I IFN response and cGAS- STING pathway

Type I interferons (IFNs) are potent inducers of the first-line defense against pathogens. Their activity leads to the up- and downregulation of a plethora of genes with various effects on the immune system, including direct effects on the pathogens. Cytosolic PRRs that recognize nucleic acids from viruses are the predominant receptors responsible for type I IFN production in most cells. A DNA sensor that mainly involved in the induction of type I IFN response, called cGAS (Cyclic guanosine monophosphate (GMP)–adenosine monophosphate (AMP) synthase) (Sok et al., 2018; Bai et al.,20019) . Cytosolic DNA (double- stranded DNA) can bind to cGAS in a sequence independent manner, promoting a conformational change of the catalytic center of this sensor. Now, cGAS, in presence of ATP, converts GTP (guanosine triphosphate) into a second messenger cGAMP (cyclic GMP-AMP). The second messenger cGAMP binds to STING (Stimulator of IFN genes), leading to a conformational change, which in turn, induces the translocation of STING from the ER- endoplasmic reticulum (where normally is located) to Golgi apparatus. Then, STING recruits TBK1 (TANK-binding kinase 1), which phosphorylates IRF3 (interferon regulatory factor 3). IRF3 binds to interferon-stimulated responsive elements (ISRE) in the nucleus leading to IFN-α/β production. STING can also recruit IKK (IkB kinase), which subsequently activates IkB (inhibitor of kB) via phosphorylation leading to the NF-kB release from the cytoplasm and translocation to the nucleus, inducing the production of proinflammatory cytokines (some studies suggest that NF-kB activation enhances also the type I IFN production) (Barber, 2011). Recent studies have revealed that phosphorylation of STING by the TBK1 is necessary for IRF3 recruitment through its conserved, positively charged phospho-binding domain with subsequently IRF3 phosphorylation by TBK1 (Liu., 2015; Zhang et al., 2019)

IFN-α (more than 10 closely related genes), IFN-β, IFN-ε-τ, IFN-κ, IFN-ω (in humans) and limitin/IFN-ζ (probably more than 10 genes in mice) are collectively called type I IFNs, and they are the largest class of IFNs. The receptor (IFNAR) is common for all the subtypes of type I IFNs. IFNAR is expressed by nearly all cell types, including the endocrine, immune, and central nervous system (glia and neurons). Type I IFNs were found to systemically activate not only natural killer (NK) cell activity, but also, other cells of the immune system, such as antigen-presenting dendritic cells (DC), T cells and B cells (Crow et al., 2015). Interestingly, type I IFN receptor levels vary on hematopoietic cells, with monocytes and B cells expressing the highest level. Adenoviral infection causes intense B cell response to type I IFNs, including early B cell activation, germinal center formation, Ig isotype switching as well as plasma cell differentiation (Domeier et al.,2018; Pogue et al., 2004; Zhu et al.,2007). Several studies have shown that IFN response is crucial for the brain homeostasis and neuronal cells can be both type I IFN producers and IFN responding cells. Neurons can respond to type I IFNs by expressing ISGs that make the cell resistant to subsequent infection (Paul et al., 2007).

IFNAR is consists of two chains, interferon-alpha/beta receptor (IFNAR) 1 and IFNAR2. IFNAR1 is constitutively associated with TYK2 (tyrosine kinase 2), whereas IFNAR2 is associated with JAK1 (Janus kinase 1). Once type I IFNs bind to their receptor, the outcome is the dimerization of the receptor subunits, leading to phosphorylation of TYK2 and JAK1, creating docking sites for STATs. JAK/STAT signaling pathway leads to the transcriptional upregulation of a numerous of interferon stimulated genes (ISGs), with antiviral, antiproliferative or immunomodulatory roles. Some ISGs are also coding for factors involved in pathogen sensing and in IFN production, creating a positive feedback loop for IFN production. It has been found that several genes, after IFN stimulation pathway, are involved in apoptosis, a form of programmed

cell death (Kaminskyy et al., 2010). Although there are pathways that link IFN signaling and cell death, the mechanism of their action remains unclear (Hervas-Stubbs et al., 2011)

1.7.2 Accumulation of cytoplasmic DNA triggers type I IFN response through cGAS-STING pathway

Nuclear DNA damage can cause specific structures within which chromosomes are found, called micronuclei. The source of micronuclei is the deficient bipolar chromosome segregation during cell division. The chromosome failing to partition into the new nuclei, will form micronuclei. Micronuclei (are stained positive for γH2AX, a DNA damage marker) are surrounded by nuclear envelope, but the whole structure is prone to rupture. Once nuclear envelope is ruptured, DNA content is released to the cytoplasm. There, cytoplasmic DNA can bind to cGAS, activate STING pathway with subsequently production of type I IFNs and other proinflammatory cytokines. During mitosis, cGAS is associated with chromosomes, but still inactive. Activation of cGAS by chromatin fragments within the micronuclei must be further assessed. Little is known about the mechanism for translocating DNA fragments from the nucleus to the cytoplasm. There is evidence that MUS81 (is an endonuclease that resolves interstrand DNA lesions) is implicated in the conversion of nuclear DNA to cytoplasmic DNA (Li et al., 2018; Harding et al., 2017).

According to Rello- Varona et al., 2012, a small portion of observed micronuclei are surrounded by double membrane vesicles and are stained positive for LC3 and p62/SQSTM1 (markers of autophagosomes) and LAMP2 (lysosomal marker), suggesting the autophagy involvement in sequestration and degradation of micronuclei. Both the envelope and chromatin are autophagic substances (figure 6).

Autophagy is a self-digesting mechanism of the cell that removes unnecessary or dysfunctional components. Autophagy initiation demands the activation of a pre-initiation complex. This complex comprises of the factors ULK1/2, ATG13 & FIP200, it is important for phagophore nucleation and its role is to activate a downstream complex that bares PI3K Class III activity. This complex consists of VSP34 Beclin 1 and UVRAG or Atg13. Though this PI3K complex, the generation of PIP3 is assisted. The newly formed phagophore becomes gradually decorated with PI3P. This molecule serves as a signal for the activation of proteins with ubiquitin like activities, ATG5-12-16L and LC3II complexes, which help the stabilization and targeting of the elongating vesicle alike. Sequestosome 1 (SQSTM1/p62) is an autophagy receptor, recognizing ubiquitinated cargo and linking cargo to the nascent autophagosome (selective substrate for autophagy). LC3II is crucial for this pathway as it sequestrates autophagosome towards fusion with the lysosome. Ultimately, the autophagosome fuses with lysosome, forming the autolysosome. This compartment is equipped with many hydrolytic molecules that degrade materials and release basic molecules like amino acids and nucleotides. These materials are recycled and reused for the formation of other cellular structures (Papandreou., 2019).

Micronuclear autophagy (autophagic removal of micronuclei) has been described as one type of nuclear autophagy. There is another type of nuclear autophagy in mammalian cells, called macronucleophagy (Luo et al., 2016). Nuclear materials, such as DNA, are encapsulated by the nuclear membrane. In this process, the formation of the nuclear autophagosome is based on the interaction of two proteins, LC3B-II, which is present in the nucleus, and LAMINB1, which is located next to inner nuclear membrane (figure 6, Luo et al., 2016). Furthermore, LC3B-II binds, through its interaction with LAMINB1, to lamin-associated domains (LADs) on chromatin. Consequently, the nuclear autophagosome is composed of, among the other

materials, LAMINB1, nuclear envelope and chromatin fragments (Dou et al., 2015). LC3BII-LAMINB1 interaction is present under basal conditions, but aberrant cellular activities trigger autophagosome formation and lysosomal degradation, may driving senescence (Leidal et al., 2015).

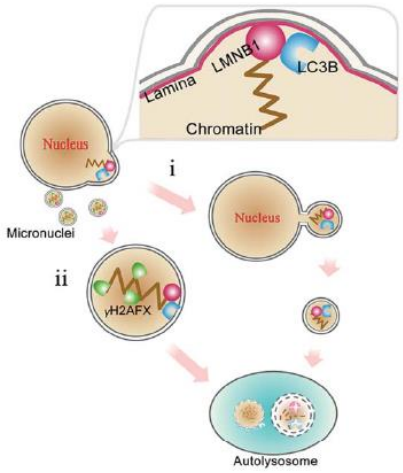

Figure 6: Two distinct types of nuclear autophagy

Another study suggests that, after downregulation of nuclear LAMINB1 (nuclear envelope disruption), the hallmark of senescence, nuclear-to-cytoplasm chromatin blebbing is occurred (Ivanov et al., 2013). Cytoplasmic chromatin fragments are positive for γH2AX, and heterochromatin markers H3K9me3 and H3K27me3, but negative for LAMINB1. CCFs activate the cGAS/STING pathway, promoting the senescence-associated secretory phenotype (SASP) (Glück et al., 2017; Dou et al., 2017). In the cytoplasm, CCFs may be substrates for the autophagy-lysosomal pathway, as indicating by the co-localization of autophagy related markers. Studies have shown that treated cells with chemical agents, such as etoposide and cytosine arabinoside (Ara-C), present accumulation of cytoplasmic DNA, due to DNA damage, and subsequently activation of the immune system (through the cGAS/STING pathway). The presence of cytoplasmic damaged DNA is reduced after B- leptomycin treatment, which blocks the nuclear transport to the cytoplasm (Lan et al., 2018). There is a hence evidence that autophagy/lysosomal pathway plays a major role in the cytoplasmic DNA clearance. The amount of cytosolic DNA is reduced after rapamycin treatment, an inducer of autophagy. Consequently, all these observations indicate an innate immune response in cells, which is cGAS/STING-dependent and is affected by autophagy and lysosomal activity.

Since the cytoplasmic DNA is processed by autophagy/lysosomal pathway, it is not clearly understood how DNA can be sensed by cytoplasmic DNA sensors. Deficiencies in autophagy/lysosomal machinery may result in increased presence of DNA in the cytoplasm witch, in turn activates innate immunity. In mice deficient for the lysosomal nuclease Dnase2a, cytoplasmic DNA levels were increased, and the undegraded damaged DNA was sensed cytoplasmic DNA sensors- STING pathway (Lan et al., 2018). In addition, Gkirtzimanaki et al., 2018, suggest that sustained IFNα signaling leads to impairment of autophagy machinery, through lysosomal alkalinization. As a result, accumulated DNA in the cytoplasm in parallel with IFNα signaling, promotes an anti-viral like response through cytosolic STING sensing pathway. All together reveal a link between cytoplasmic DNA, autophagy/ lysosomal pathway and inflammatory response, but the detailed mechanism responsible for this link must be elucidated.

1.8 Microglia, brain-resident immune cells

1.8.1 Microglia in normal conditions

Microglia are brain-resident myeloid cells that mediate key functions to support the CNS. Microglia cells express a wide range of receptors that act as molecular sensors, which recognize exogenous or endogenous CNS insults and initiate an immune response. In addition to their classical immune cell function, microglia act as guardians of the brain by promoting phagocytic clearance and providing trophic support to ensure tissue repair and maintain cerebral homeostasis. Microglia constitute 5%–12% of all glial cells in the rodent brain and 0.5%–16% in humans. Microglia originate from the yolk sac during primitive hematopoiesis (Gordon et al., 2005). The brain maintains microglia levels via a finely tuned balance between local proliferation and apoptosis, without contributions from peripheral monocytes.

As the brain's resident immune cells, microglia participate in the establishment of normal neuronal connectivity and regulatory processes critical for CNS development, such as synaptic pruning, which ensures elimination of inappropriate synapses to strengthen the appropriate ones based on neuronal activity and experience. microglia play an important role in maintaining homeostasis by removing cellular debris, dying cells, or misfolded protein. In the adult brain, microglia are involved in modulating higher cognitive functions such as learning and memory. Resting microglia actively monitor the CNS parenchyma, and this surveillant phenotype in combination with a specific receptor repertoire facilitates rapid microglial responses to changes in the microenvironment (figure 7, Derecki et al., 2013).

Microglia express many pattern-recognition receptors (PRRs) that detect pathogen-associated molecular patterns (PAMPs) or tissue damage–associated molecular patterns (DAMPs). Microglial PRRs include Toll-like receptors (TLRs), such as TLR4 and TLR1/2, and their coreceptors, such as CD14, NOD-like receptors (NLRs), such as the NLRP3 inflammasome receptors for nucleic acids and C-type lectin receptors (CLRs), such as CLEC7A. Microglia express chemokine receptors, such as CX3CR1 and CXCR4, as well as integrins, such as CD11b and CD11c, that control migration and positioning of microglia within the CNS and enhance their capacity to bind target cells to be phagocytosed and eliminated. In addition to immune receptors, microglia express multiple receptors for neurotransmitters and neuropeptides released by neurons that promote neural-glia communications. These receptors allow microglia to monitor neuronal activity by guiding microglia processes toward neuronal synapses in order to influence synaptic plasticity and sculpt dendritic spine density. Microglia express various purinergic receptors for ATP, such as P2Y12 and P2X7. P2Y12 is active in resting microglia but downregulated upon activation and it drives migration and phagocytosis (Rivest et al., 2009).

Histologically, CNS-resident microglia are indistinguishable from blood-derived macrophages that acutely infiltrate the CNS in response to pathogenic insult. Both myeloid cell types express classic macrophage markers (Iba-1, F4/80, and mac-1) and both cell types are inducible for MHC and co-stimulatory molecules (B7.1, B7.2, and CD40) required for antigen-dependent activation of T cells. Interestingly, two seminal studies demonstrated that CNS resident microglia are not identical to macrophages that acutely infiltrate the CNS. In the first study, (Hickey et al., 1988) it was observed that local proliferation alone can maintain the number of microglia with little or no recruitment from the blood to the brain parenchyma. In the second study, (Sedgwick et al., 1991) it was discovered that in contrast to peripheral macrophages, parenchymal microglia expressed much lower levels of CD45, a protein tyrosine phosphatase expressed by all nucleated cells of hemopoietic lineage.

1.8.2 Microglia in pathological conditions

According, the classification of macrophages, there are two distinct types, M1-proinflammatory and M2- anti-inflammatory. M1 phenotype is characterized by production of cytokines and chemokines (IL-1β, IL-6, IL-12, TNF-α, CCL2), expression of NADPH oxidase, generation of reactive oxygen and nitrogen species and production of inducible nitric oxide synthase (iNOS), leading to potential damage via reactive nitrogen species . M2 phenotype is characterized by M2 microglia produce anti-inflammatory cytokines (IL-10, TGF-β), growth factors (IGF-1, FGF, CSF1), and neurotrophic growth factors (nerve-derived growth factor [NGF], brain-derived neurotrophic factor [BDNF], neurotrophins, glial cell–derived neurotrophic factor (GDNF). However, transcriptome analysis of microglia derived from models of neurodegenerative diseases failed to show any clear M1 or M2 signature. Instead, they found simultaneous expression of both M1 and M2 markers, suggesting the presence of mixed phenotypes (Sarlus et al., 2017).

As the primary source of proinflammatory cytokines, microglia are pivotal mediators of neuroinflammation and can induce or modulate a broad spectrum of cellular responses (Perry et al., 2013). Alterations in microglia functionality are implicated in brain development and aging, as well as in neurodegeneration. When microglial functions are impaired, the CNS can become fertile ground for acute or chronic pathologic processes. Under inflammatory conditions, the vascularization of the CNS is the basis for microglial distribution and the recruitment of monocytes and adaptive immunity cells from the circulation. The process of microglia migration to the damage site and the proliferation in acute injury and chronic neuronal diseases is called reactive microgliosis; is rare and tightly regulated (González et al., 2014). Following the clearance phase of the damaged site, microglial cells also provide reparative functions and stimulate astrogliosis for and tissue reformation. Finally, activated phagocytic cells are believed to adapt again their ramified quiescent form.

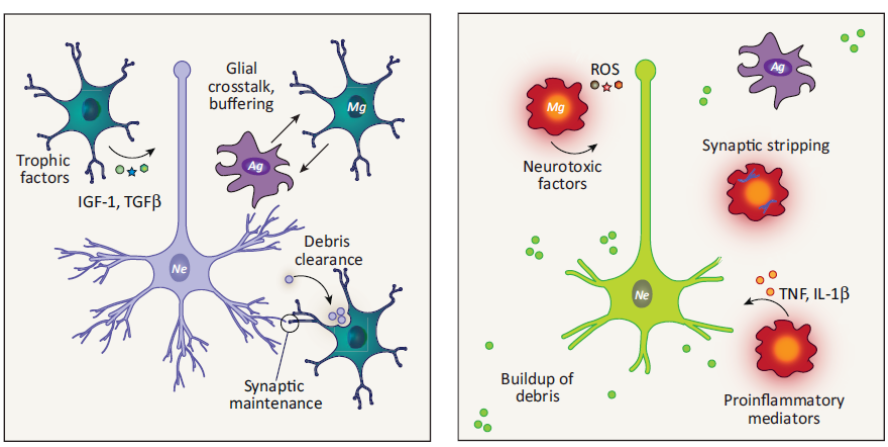

Figure 7: Microglia functions in the healthy and diseased CNS.

1.8.3 Microglia in the aged brain

Local proliferation alone can maintain the number of microglia with little or no recruitment from the blood to the brain parenchyma. The increased inflammation in the aged brain is attributed, in part, to the resident population of microglia. Microglia of the aged brain are marked by dystrophic morphology, elevated expression of inflammatory markers, and diminished expression of neuroprotective factors (Niraula et al., 2017). Importantly, the heightened inflammatory profile of microglia in aging is associated with a 'sensitized' or 'primed' phenotype. There is a causal link between the primed profile of the aged brain and vulnerability to secondary insults, including infections and psychological stress. Primed

microglia are characterized by an exaggerated and uncontrolled inflammatory response to an immune stimulus. When primed microglia are triggered by proinflammatory stimuli, they become hyper-reactive, secreting large amounts of cytokines, chemokines, and other reactive molecules associated with neurotoxicity (Holtman et al., 2015). Microglia priming is also evident in CNS pathologies. The CNS microenvironment has a profound effect on the microglial phenotype. Ligands expressed by neurons, astrocytes or oligodendrocytes bind receptors expressed on microglia, and signaling through these receptors inhibits the activation of microglia, such as CD2000–CD200R116 and CX3CL1–CX3CR1 (Rivest et al., 2009). Neuronal damage or degeneration leads to loss or downregulation of neuronal ligands that bind to inhibitory receptors on the microglia, thereby releasing microglia from inhibition.

Raj et al., 2014, suggest that microglia are primed in a DNA-repair deficient model of accelerated aging (Ercc1Δ/KO). In WT brain, microglia extended thin ramified processes, whereas in Ercc1Δ/KO mice microglia possessed hypertrophic, thickened processes, and enlarged cell bodies. Furthermore, increased microglia proliferation, enhanced sensitivity to LPS stimulation, increased phagocytosis and reactive oxygen species (ROS) production and enriched for "antigen presentation" pathways are main characteristics observed in Ercc1Δ/KO mice.

Antigen presentation is a key event in the initiation and development of T cell-mediated immune responses. MHC class II molecules (MHC II) present peptide antigens derived mostly from endogenous and exogenous proteins that access the endocytic route, where they are degraded. Simultaneous recognition of a specific major histocompatibility complex (MHC)–peptide complex by the T-cell receptor (TCR) and of CD80 or CD86 by the co-stimulatory receptor CD28 results in T-cell activation, cytokine production, proliferation and differentiation. In the absence of CD28 ligation, T cells undergo apoptosis or become anergic. After T-cell activation and upregulation of cytotoxic T-lymphocyte antigen 4 (CTLA-4; CD152), co-ligation of the TCR and CTLA-4 results in cell-cycle arrest and termination of T-cell activation (Alegre et al., 2001).

The gene expression networks of primed microglia in four different mouse models of aging and neurodegeneration (1) aged mice, 2) accelerated aging mice (Ercc1Δ/KO), a DNA repair-deficient mouse model that displays features of accelerated aging, 3) a mouse model for Alzheimer's disease and 4) a mouse model for Amyotrophic Lateral Sclerosis) were compared acute activated microglia followed LPS treatment. The primed microglia and the acute LPS-activated microglia were most strongly enriched for "immune response" and "response to stress" pathways. The primed microglia were significantly enriched for "antigen presentation", "Alzheimer's disease signaling", "lysosome" and "phagosome" pathways. On the other hand, the acute LPS-activated microglia were enriched for "Toll-Like Receptor (TLR) signaling", "NOD-like receptor (NLR) signaling" and "ribosome" pathways (Holtman et al., 2015).

1.9 Purkinje cells-neurons

Purkinje cells are large neurons located exclusively in the cerebellum. Purkinje cell bodies are shaped like a flask and characterized by a lot of branching dendrites and a single long axon. These neurons are the only output of the cerebellar cortex. Purkinje cells release the GABA (gamma-aminobutyric acid) neurotransmitter and play a crucial role to neuronal circuit in the brain. These inhibitory functions enable Purkinje cells to regulate and coordinate motor movements (Brown et al., 2018). Severe neurological diseases are caused by Purkinje cell degeneration. A well- described disease implicating the loss of Purkinje cells is the cerebellar

ataxia. Cerebellar ataxia is one of the most devastating symptoms of Ataxia-Telangiectasia (A-T), among others like telangiectasia, immunodeficiency, cancer susceptibility and radiation sensitivity (Rothblum-Oviatt et al., 2016).

Microglia and neurons are in constant interaction. Cerebellar microglia make dynamic contacts with Purkinje neuron dendrites and somas and respond rapidly to focal laser injury. Microglial cell somas were interspersed between the Purkinje neuron somas and could be observed moving around the cells effectively forming a C-shape wrapped around the neuronal. Additionally, microglial processes often wrapped around, and remained in proximity with Purkinje cell somas as they retracted and extended. Most microglial arbors were in contact with 4–8 Purkinje neuron somas at any one time. Such robust interactions and monitoring of multiple somas simultaneously could allow microglia to respond to changes in neural activity associated with plasticity or damage (Stowell et al., 2018).

1.10 Exosomes in the Central Nervous System (CNS)

1.10.1 Exosomes- an overview

Intercellular communication plays a crucial role in the maintenance of cellular functions and tissue homeostasis in organisms. This communication is occurred either through direct cell-cell interaction or via secretory molecules. All type of cells secretes extracellular vesicles containing a variety of macromolecules facilitating the cell signaling (Gurunathan et al., 2019). Exosomes are one kind of these extracellular vesicles, originating from the endocytic pathway. Their size varies from 30 to 150 nm in diameter and are enriched for specific markers. Exosomes are formed as intraluminal vesicles (ILVs) in the multivesicular bodies (MVBs). ILVs have three distinct destinations, they can degrade, recycle or exocytose their content. Last one is performed after fusion of the outer MVB membrane to the plasma membrane. Exosome cargo consists of proteins, sugars, lipids and a variety of genetic materials, protected from extracellular proteases and nucleases by the limiting membrane (figure 8, Gurunathan et al., 2019). These membrane-bound vesicles can be internalized via endocytosis or membrane fusion with subsequently releasing their contents to recipient cells for cargo utilization or degradation (Mathieu et al., 2019).

Biological functions of exosomes are determined by the donor cell and the status of the originating tissue or cell at the time of exosome generation. Exosomes are implicated in a various of processes like angiogenesis, apoptosis, antigen presentation, inflammation, cell proliferation and differentiation and can be used as remarkable biomarkers for a wide range of diseases diagnosis. Furthermore, exosomes have therapeutic applications based on their properties. For instance, exosomes can distribute over short and long distances, cross tissue barriers (e.g. BBB), have the ability to protect their contents and have the potential to deliver cargo to specific cell types through ligand-receptor interactions. Within the nervous system, exosomes have an emerging role not only at the physiological state, but also in pathological conditions. Exosomes round off communication in the brain (Budnik et al., 2016). Several studies reveal the role of exosomes in brain cells communication, such as neuron-neuron interactions, glia (microglia, astrocytes and oligodendrocytes)- neuron interactions, as well as glia-glia interactions. In neurodegenerative diseases, like Alzheimer disease, beta-amyloid peptides (protein aggregates) are carried out by exosomes in a neuroprotective/ neurotoxic manner (Miranda et al., 2018). Propagation of misfolding proteins to neighboring cells, and therefore disease propagation is mediated by exosomes (Abdulrahman et al., 2018).

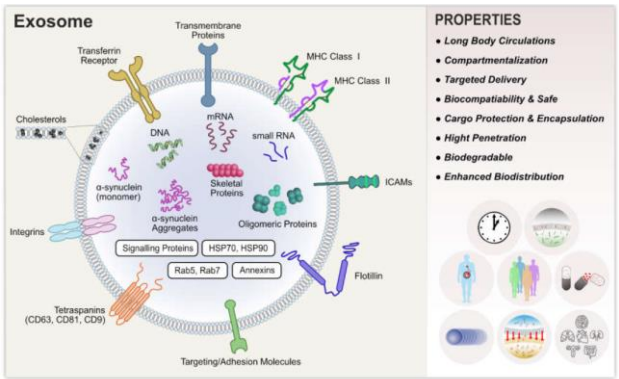

Figure 8: Exosomal proteins and properties

1.10.2 Autophagy–exosome crosstalk

The eukaryotic endomembrane system is a complex system containing membrane-bound organelles participated in a numerous of cell processes in due to maintain cell homeostasis. Exosomes and autophagy, a lysosomal-dependent pathway, are two core components of this system. There is a constant interplay between exosomes and autophagy, as indicating by the contribution of autophagy-related proteins to exosome biogenesis and release (Baixauli et al., 2014). For instance, in ATG5 ko cells, MVB fusion to the plasma membrane resulting in exosome release is favored over the MVB-lysosome fusion and cargo degradation.

Additionally, it has described an alternative fate pathway for both MVB and autophagosomes. Autophagosomes can fuse with MVBs, creating a hybrid vesicle, called amphisome (figure 9, Xu et al., 2018). Amphisomes have the ability either to fuse with lysosomes for cargo degradation or fuse with the plasma membrane for secretion of their content. This is the way that cytosolic annexin 2 (ANXA2) is secreted in exosomes. As mentioned before, neurons utilize exosome release in due to eliminate protein aggregates (reduced neurotoxicity). However, the autophagy machinery is, also, used for this purpose. Studies have shown that when autophagy/lysosomal pathway is impairment, exosome release may be enhanced to stress relief. Hessvik et al., 2016 propose that impaired fusion of lysosomes with both MVBs and autophagosomes, increases the fusion between MVBs and autophagosomes, generating amphisomes. After apilimod treatment (PIKfyve inhibition leading to impaired fusion of lysosomes with both MVBs and autophagosomes), the number of released particles was elevated, but the size distribution of these particles was the same. Also, autophagy-related proteins like p62 and LC3 were observed in the exosomal fraction. In conclusion, PIKfyve increases secretion of exosomes and induces secretory autophagy, indicating that these pathways are closely linked.

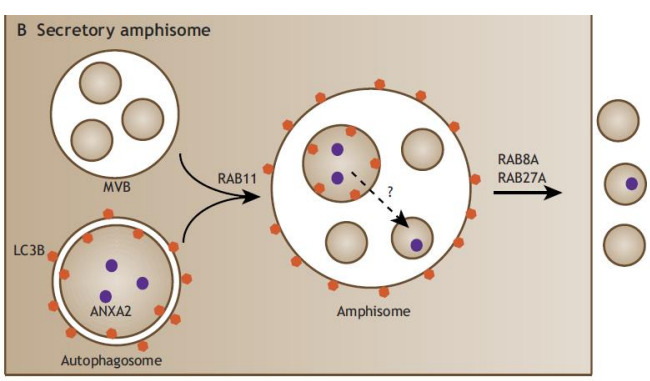

Figure 9: Emerging interplay between autophagy and exosomes

Aim of the study

In this study we examine whether the microglia- specific DNA damage accumulation is enough to drive age- related neuropathology.

Chapter II:

Materials and Methods

Methods

2.1 Microglia adult mouse brain - Percoll Isolation

Briefly, brains were removed from the skull and placed in 50 ml tubes with standard ice-cold medium (DMEM 10% FBS, 1% PSG), followed by two same medium washes. Tissue was placed in 1x PBS and minced into <2 mm pieces. Cell suspension was packed by short spin centrifugation and the pellet was resuspended in collagenase mix*.

Two commonly used procedures: enzymatic digestion and mechanical dissociation were used to isolate CNS microglia until the acquirement of single cell suspension. More specifically, the pieces of tissue were incubated in collagenase solution for 40-45 min at 37^{o}C and were gently triturated every 5 minutes. Collagenase activity was halted by adding 10 ml medium to the resultant homogenate.

Cells were suspended in ice-cold medium, centrifuged 5 min at 280g, 18^{o}C twice and the supernatant was cautiously discarded. Cell suspension was further homogenized using a syringe (21G needle) and filtered through a sterile pre-moistened 40 μm cell strainer to separate the clumped cells, meninges and tissue fragments from the larger pieces. Follows resuspension in ice-cold medium and a 5-min centrifugation step.

The supernatant was discarded and the pellet of brain was resuspended in 2.5 -3 ml of 75% isotonic Percoll (high Percoll) into a 15mL polystyrene tube. On top of high Percoll 5 ml of 35% isotonic Percoll (low Percoll) was layered, followed by 1 ml of 1x PBS. The gradient was then centrifuged at 800*g* for 40 minutes, 4°C, low acceleration and no brake.

Samples should be processed immediately after centrifugation to avoid a lesser yield. A thin band of desirable cells was captured between low and high Percoll layers. Two ml of interphase (microglia + lymphocytes) were collected and diluted with 1x PBS more than three times, in order to lessen the contact of cells with Percoll. The diluted homogenate was vigorously agitated and finally was spun at 1000 *g* for 10 minutes at 4°C, full acceleration and brake. A final Washing-Centrifugation Step is recommended in 500 μl medium volume, 800g, 7 min at 4C and transferred into 1.5-mL Eppendorf tubes.

The pellets of Isolated cells were suspended in DMEM that included 10% FBS 1 %PSG (100 units/ml) and were placed on un-coated glass coverslips in a 24-well plate.

2.2 Culture Preparation

In order to compare the functional responses of adult brains, microglial cells were seeded in a 24-well tissue culture plate (Costar) at a density of >50.000 cells per well. Cultures were incubated at 37°C with 5% CO2 and the medium was changed every three days, to remove cell debris, released inflammatory or apoptotic factors and avoid a higher apoptotic rate.

2.3 Microglial cell isolation using CD11b MicroBeads – MACS Miltenyia

2.4 Brain cryosections immunochemistry

Tissue Sections were removed from -20^{o}C and were defined using Dako-Pen. They were incubated at RT for 5 minutes. The samples were further incubated in Glycine, for 5 min, RT. Three washing steps followed with 1X PBS, for 6min, at RT and blocking in a solution of 0.01% Digitonin in 1X PBS at RT, for 45-60 minutes. Then, the primary antibody solution was placed overnight at 4^{o}C. Samples were immunostained with the corresponding fluorescent-labeled antibodies for 2 hours, at RT. A separate 10-minute incubation was carried out in DAPI and the slides were coverslipped with 80% Glycerol. Three 6 min washes with a solution of 0.2% Triton in 1X PBS were performed between the incubations.

2.5 Immunochemistry on microglia cells

Microgia cells placed on coverslips were fixated with 4% F/A for 15' maximum, RT. Then the coverslips were places on a Petri dish covered with parafilm (hydrophobic) and washed 3X wirh 1X PBS, for 5', RT. Permeabilization/Blocking was performed by using B1 solution (1% BSA, 0,5%Triton), for 1h, RT. Once blocking was done, primary antibodies in B1 solution were added on the coverslips, O/N, at 4oC. The following day, coverslips were washed three times with B2 solution (0,5% Triton in 1X PBS), 10', RT and secondary antibodies were added, along with DAPI. Finally, coverslips were washed again, three times, with B2, 10', RT and then they were put on microscope slides with 80% glycerol. At this stage, microglia cells are ready to be observed by confocal microscopy.

2.6 Western blot analysis of protein samples

Gels were prepared by mixing acrylamide (30%) with the appropriate amount of separating/stacking gel buffers and polymerization was induced after the addition of 10% ammonium persulfate (APS) and TEMED® reagents. 1.5M Tris (pH 8.8) and 1M Tris (pH 6.8) were used as the buffers for the separating and the stacking phase of the gel, respectively. After quantitation of the protein concentration, 15 ug of each protein sample were used for western blot analysis. After the addition of Loading dye (at a final concentration 1x), samples were heated at 96oC for 3 minutes, spanned down and loaded onto polyacrilamide gel. For the indication of molecular weight of proteins, 7uL of protein ladder were used. Electrophoresis of samples was performed at 80V while proteins moved through the stacking phase, and then at 100-120V in the separating phase of the gel. After approximately an hour, electrophoresis was stopped and proteins were transferred from gels to activated PVDF membranes (soaked in methanol for 1-2 minutes), in transfer buffer (2.9g Glycine, 5.8g Tris base, 0.37g SDS, 200ml methanol) at a constant current of 400mA. After transfer process, membranes were briefly washed in PBST buffer (phosphate buffered saline with Tween® 20, 0,1%), then blocked in 5% skimmed milk diluted in PBST for 1 hour. Membranes were washed again and incubated with the primary antibodies overnight at 4oC. Afterwards, membranes were washed briefly in PBST and incubated at room temperature with the secondary antibody for 1 hour. Brief washes with PBST were performed to remove unbound secondary antibody molecules and enhanced chemiluminescent (ECL) peroxidase substrate was used. Samples were normalized using antibodies for housekeeping genes (β-tubulin).

2.7 RNA extraction

RNA-extraction was performed using TRIzol reagent. Cells from 60mm cell culture well plate were extracted in 500ul of Trizol. 1/5 of the initial trizol volume of chloroform was added, mixed well and centrifuges at 12000g for 15 minutes. The upper phase was collected into a new tube and ½ of the initial volume of 2-propanol was added for the precipitation to happen. A centrifugation followd 12000g for 15 minutes and the pellet was washed with 70% EtOH, 7500g 5minutes. The pellet was resuspended in 10-20ul of water.

2.8 cDNA synthesis

cDNA synthesis was performed using minotech-RT reverse transcriptase and protocol. Briefly, a mixture of 1 µl of oligo(dT)20 (100 µM), 10 ng–2 µg total RNA, 1 µl 10 mM dNTP Mix (10 mM each dATP, dGTP, dCTP and dTTP at neutral pH) and Sterile ultrapure water up to 13 µl was heated at 65C for 5 minutes. The mixture was incubated at 4C for 2 minutes and 4 µl 5X MINOTECH RT assay buffer, 1 µl 0.1 M DTT, 1 µl RNase Inhibitor (40 units/µl) and 1 µl of MINOTECH RT (~200 units/µl) were added. After being mixed gently the mixture was incubated at 42C for 60minutes and a heat inactivation step at 70C for 15 minutes followed.

2.9 qRT- PCR

Quantitative PCR (Q-PCR) was performed with a CFX Connect Real-Time PCR Detection system device according to the instructions of the manufacturer (BIO RAD). The generation of specific PCR products was confirmed by melting curve analysis. Hypoxanthine guanine phosphoribosyltransferase1 (Hprt-1) mRNA was used as an external standard. The primers that were used for qRT-PCR are:

2.10 Flow cytometry

Whole brains from wt and ko mice were isolated and treated with collagenase (as described in **2.1).** After that, cells were stained with fluorochrome conjugated and unconjugated antibodies for 15-20 min at 4C in PBS/5% FBS. Also, Annexin V/PI kit was used. Similarly, exosomes isolated as described in **2.12**, were analyzed by FACs analysis. Samples were acquired on a FACS Calibur (BD Biosciences) and analyzed using the FlowJo software.

2.11 B16-Blue IFN- α/β cells

2.11.1. Initial culture procedure

The vial containing the cells gets thawed by gentle agitation in a 37oC waterbath. Once the contents were thawed the vial was removed and then sprayed with 70% ethanol. Cells were transferred in a larger vial containing 15ml of pre-warmed growth medium (DMEM, 10% (v/v) heat-inactivated FBS, 100 U/ml penicillin, 100 µg/ml streptomycin, 100 µg/ml Normocin, 2mM L-glutamine). No selective antibiotics were added at that point, since cells have to be passaged twice before antibiotics' addition. Moving on, the 15ml vial containing the cells, was centrifuged at 300g for 5', supernatant was discarded and the pellet (cells) was resuspended with 1ml of growth medium without selective antibiotics. Finally, the vial contents were transferred to a T-25 tissue culture flask containing 5ml of growth medium without selective antibiotics and then placed at 37oC, in 5% CO2.

2.11.2. Frozen stock preparation

Cells were resuspended at a density of 3-5x106 cells/ml in a freezing medium (DMEM, 20% FBS, 10% (v/v) DMSO) prepared extemporaneously with cold growth medium. One ml of cells

was aliquoted into cryogenic vials and placed in a freezing container. Vials were stored at -80oC overnight and then transferred to liquid nitrogen for long term storage.

2.11.3. Cell Maintenance

Cells were maintained and subcultured in growth medium supplemented with 100 μg/ml of Zeocin. Growth medium was renewed twice a week and cells were checked every day. Cells were ready to be passaged when a 70-80% confluency was reached. It is important that the cells do not grow to 100% confluency.

2.11.4. Reporter Assay

A cell suspension of B16-Blue cells was prepared. This suspension contained 420.000 cells/ml in growth medium. Almost 75.000 cells in growth medium were added per well (24 well plate), along with culture media (stored at -80oC) from previous experiments. The plate was incubated at 37% in 5% CO2 overnight. The next day, QUANTI-Blue solution (1ml QB reagent, 1ml QB Buffer and 98ml sterile water) was prepared and added in each well of a 96 well plate. Moreover, duplicates of induced B16-Blue cells' supernatants were added, along with a positive (murine IFNalpha) and negative control (growth medium). The plate was incubated at 37oC for 3h. After that 3h incubation SEAP levels were determined using a spectrophotometer at 620-655 nm.

2.12 Exosome isolation

Whole brains from wt and ko mice were isolated and treated with collagenase (as described in **2.1).** Brain parenchyma before and after collagenase treatment was kept for exosome isolation.

2.12.1 Preparation of crude exosome pellet by differential ultracentrifugation

- Collect x ml of culture medium into 50-ml conical tubes and centrifuge at 4°C (1,000 g for 10 min) to remove intact cells.
- Pipet off the supernatant, transfer it to fresh 50-ml conical tubes, and centrifuge at 4°C (2,000 g for 20 min) to remove cell debris.
- Pipet off the supernatant, transfer it to fresh 50-ml conical tubes, and centrifuge at 4°C (10,000 g for 30 min) to remove microvesicles.
- Pipet off the supernatant, transfer it to Beckman tubes (38.5-ml ultra-clear tubes), and ultracentrifuge at 4°C (100,000 g for 2 hour) using a SW32 Ti or equivalent rotor to remove the crude exosomes.
- Pour out the supernatant and resuspend the crude exosome pellet (100,000 g pellet) with 100μl PBS.

2.12.2 Purification of exosomes from crude exosome pellets using sucrose gradient centrifugation

- Make 10-90% sucrose stocks using PBS See figure in Figures section.
- Resuspend the crude exosome preparations (in 100μl PBS) with 1 ml 90% sucrose stock solution (final sucrose concentration = 82%). Transfer into 13.2-ml ultra-clear Beckman unltracentrifuge tubes.
- Overlay the gradient on top of the crude exosome preparation starting with 1 ml 70% sucrose solution. Technical tip: To apply sucrose solutions, place a 200 μl pipet tip on the end of a 1000 μl pipet tip containing 1 ml sucrose solution. Hold both tips steady using gloved fingers. Place the 200 μl tip in contact with the inside wall of the ultracentrifuge tube and allow gravity to feed the solutions into the tube slowly.

- Repeat step 3 with the remaining sucrose stock solutions in order from the highest to lowest sucrose concentration.
- Ultracentrifuge at 4°C (100,000g for 16 hours) in a SW41 Ti rotor or equivalent.
- Collect 2 ml fractions starting from the top to bottom. Technical tip: To collect fractions correctly without mixing the gradient, touch the side of the tube at the very top of the gradient with the end of 1000 µl pipet tip, carefully take out 1 ml and then transfer it into the Beckman tube (13.2-ml ultra-clear tube). Repeat this step again so that 2 ml fractions are collected.
- Repeat step 6 until six fractions of 2 mL each have been collected.
- Add 9mL PBS to each of the 2 ml fractions. Centrifuge at 4°C (100,000g for 1 hour) in a SW41 Ti rotor or equivalent.
- Pour out the supernatant and resuspend the pellet in 50 µl PBS. The third fraction from the top, which contains the interface of the 34% and 40% sucrose solutions, should be enriched for exosomes. The sixth fraction, which contains the interface of the 70% and 82% sucrose solutions, will contain protein/RNA/membrane aggregates.

stock solution (%)	10	16	22	28	34	40	46	52	58	64	70	90
Sucrose (g)	1.0	1.6	2.2	2.8	3.4	4.0	4.6	5.2	5.8	6.5	7.0	9.0
Add PBS to 10ml												

2.13 Electron microscopy: TEM / SEM

For transmission electron microscopy, isolated exosomes in PBS were fixated in 2% paraformaldehyde. Fixed EVs were deposited on EM grids and were further fixed with glutaraldehyde. Samples were first contrasted in a solution of uranyl oxalate and then contrasted and embedded in a mixture of 4% uranyl acetate and 2% methyl cellulose. Exosomes were examined under JEM 100C/JEOL/Japan Transmission Electron Microscope.

For scanning electron microscopy, isolated exosomes were diluted in distilled water and were deposited on glass slides. Exosomes were examined under Scanning Electron Microscope.

2.14 Fixation and Immunolabeling of mouse Acute Brain Slices (SNAPSHOT method)

2.14.1. Brain slices fixation

A 12-well tissue culture plate was attached in a water bath with tape, and we ensured that the surface of the water in the bath was contacting the bottom of the plate. Each well in the tissue culture plate in the water bath, was filled with 6 ml of PFA 15 to 20 min before fixation to ensure that the temperature of the PFA reached 80°C. The acute brain slices were transferred from the artificial cerebrospinal fluid (ACSF) to the heated PFA using a transfer pipet with the tip cut off. After exactly 2 min in heated PFA, the slices were transferred to 0.1 M PBS in a 12-well plate at room temperature (6 ml in each well), using a metal spatula with the tip bent 90°.

2.14.2. Immunolabel sections

The slices were rinced to remove any residual PFA by using a spatula to move them to new wells in 12-well plate containing 0.1 M PBS. The plate was placed on a platform rotator. The tissue was permeabilized with permeabilizing/washing solution for a minimum of 2 hr. Non-

target epitopes were blocked by incubation with blocking solution over night at RT. Primary antibodies (MitoTracker, Picogreen) were diluted to the required concentrations in staining solution and each slice was incubated with the diluted primary antibodies in a small plastic bag made by using a Manual Impulse Sealer for 6 to 10 days at 4°C on a platform rotator or a 360° rotisserie wheel. After the incubation with primary antibodies, the tissue was washed with permeabilizing/washing solution three to five times over the course of a day. Secondary antibodies were diluted to the required concentrations in staining solution and the tissue was incubated with the diluted secondary antibodies in a small plastic bag made by using a Manual Impulse Sealer for 4 to 6 days at 4°C on a platform rotator or a 360° rotisserie wheel. Fluorophores were protected from exposure to light by wrapping the bags in aluminum foil. Finally, the tissue was washed with permeabilizing/washing solution three to five times over the course of a day and then it was rinsed three to five times in PBS.
Washing/permeabilizing solution: 1 phosphate-buffered saline (PBS) tablet, 2 ml Triton X-100 (2% v/v final) and 20 ml DMSO (20% v/v final). Combine the above components in a final volume of 100 ml water. Prepare fresh for each staining and hold at 4°C.

2.14.3. Image brain slices

To image the tissue slices, we placed each slice on a microscope slide prepared with the slide, cover glasses, and Krazy Glue, using a transfer pipet with the tip cut off. A small drop of PBS was added on top of the brain slice before the placement of the cover glass over the brain slice. Finally, corn oil was added to each side of the microscope slide and imaging was performed with a two-photon scanning microscope.

2.15 Mouse model

Every protocol that needed animal usage, was approved by the FORTH Animal Ethics Committee (FEC). All mice lived in an environment free of pathogens and inside clear shoebox cages with constant temperature and humidity and 12 hr/12 hr light/dark cycle. For the experiments two types of mice were used: wild-type Cx3cr1 and knock-out Cx3cr1-Ercc1.

2.16 Materials

Antibodies: Mac-1, dsDNA, pATM, p62, LC3B, DAPI, Calbindin/PerCP, IFNAR^{PE}, MHCII^{FITC}, CD86^{PerCP}, CD11b^{APC}, Annexin V ^{FITC}, γH2AX, CD45, β-tubulin, cleaved- Caspase-3, STING, Alix, CD9, CD81.

Fluorescent dyes: picogreen, Mitotracker, propidium iodide (PI)

Primers for qPCR: forward/ reverse

HPRT: CCCAACATCAACAGGACTCC/ CGAAGTGTTGGATACAGGCC

IFNα: CTGCTGGCTGTGAGGACATA/GGCTCTCCAGACTTCTGCTC

IFNβ: TGAACTCCACCAGCAGACAG/AGATCTCTGCTCGGACCACC

ISG15: GGTGTCCGTGACTAACTCCAT/TGGAAAGGGTAAGACCGTCCT

IFIT2: AGTACAACGAGTAAGGAGTCACT/ AGGCCAGTATGTTGCACATGG

MX1: GACCATAGGGGTCTTGACCAA/ AGACTTGCTCTTTCTGAAAAGCC

IFIT1: CCAAGTGTTCCAATGCTCCT/ GGATGGAATTGCCTGCTAGA

IRF1: GGAAGGGAAGATAGCCGAAG/ GGGCTGTCAATCTCTGGTTC

IFI207: CAGGCTCAGCTTTCAGAACC/ ATTTCCTGAGGACCCCTTGT

IFI44: AACTGACTGCTCGCAATAATGT/GTAACACAGCAATGCCTCTTGT

Chapter III:

Results

3.1 Ercc1 deletion triggers increased presence of γH2AX and pATM in the nucleus and the cytoplasm of CX3CR1-Er$^{F/-}$ microglia

In order to examine the outcome of unresolved DNA damage in due to ERCC1 deficiency in CX3CR1-ER$^{F/-}$ (ko) mice, microglia cells were immune-stained with γH2Ax, phosphorylated histone H2Ax which marks the region proximal to the DNA lesion (damage marker), pATM, phosphorylated ataxia telangiectasia mutated which is recruited to DNA double-stranded breaks during DDR and Mac-1/CD11b (microglia marker) and counterstained for DAPI (by Iliana Rouska). Accumulation of γH2Ax and pATM in the nucleus of in CX3CR1-ER$^{F/-}$ (ko) cells compared to ER$^{F/+}$ (wt) indicates the persistent activation of the DDR. Surprisingly, as shown in figure 9, signal from γH2Ax and pATM proteins is detectable also in the cytoplasm. These data lead to the hypothesis that upon sustained DNA damage in CX3CR1-ER$^{F/-}$ (ko) microglia, a functional interaction between the nucleus and the cytoplasm is present.

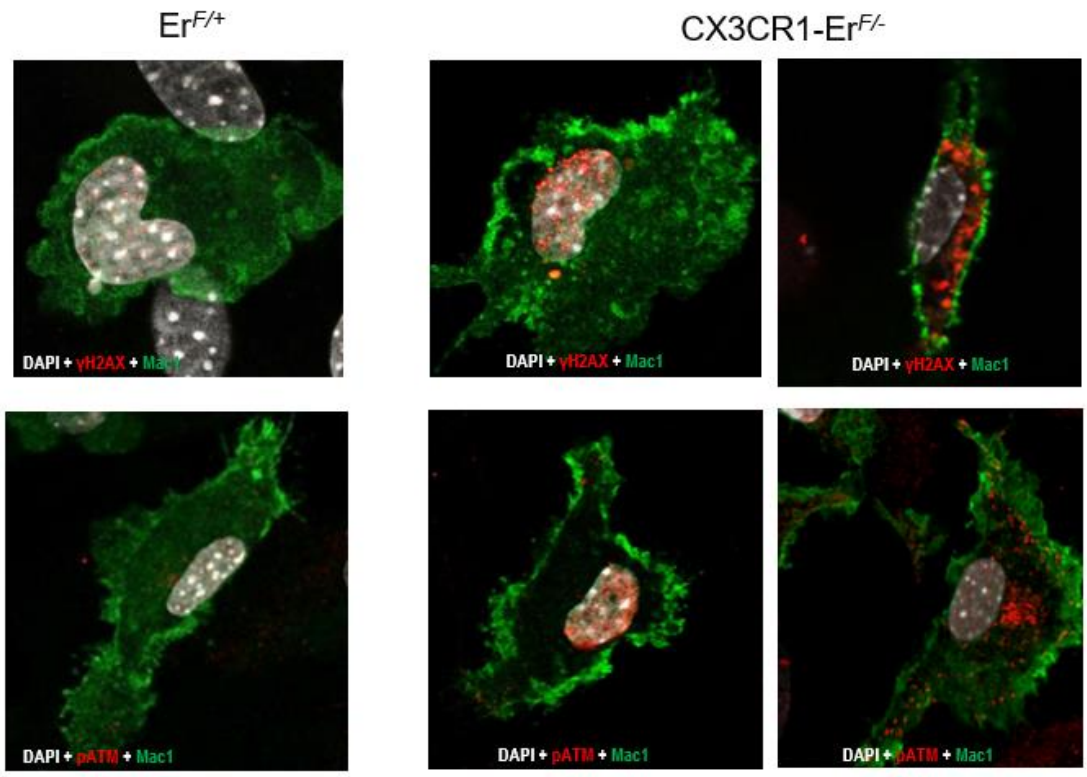

Figure 9: Persistent DDR leads to increased presence of γH2AX and pATM in the cytoplasm of CX3CR1-Er$^{F/-}$ microglia. Confocal projetions of microglia cells from CX3CR1-ER$^{F/-}$ (ko) and ER$^{F/+}$ (wt) mice were stained for Mac1-microglia marker (green), two DNA damage markers, γH2AX and pATM (red) and counterstained with DAPI (white). There is accumulation of γH2Ax and pATM in the nucleus of CX3CR1-ER$^{F/-}$ (ko) cells. Surprisingly, these proteins are also

present in the cytoplasm. Magnification x63. More mice need to be assessed to reach statistical significance.

3.2 DNA damage accumulation in microglia primes innate immune response

Preliminary observations suggest that sustained DNA damage triggers microglia activation, characterized by their highly ramified morphology. Studies have shown that in aged mice or in accelerated aging mice (Ercc1Δ/KO), microglia are associated with a 'sensitized' or 'primed' phenotype. For this reason, we examined microglia phenotype in our model mice. Expression of MHCII and CD86 (co- stimulator molecule) was measured by flow cytometry in freshly isolated microglia cells from CX3CR1-ER$^{F/-}$ (ko) and ER$^{F/+}$ (wt) mice. As shown in figure 10, there is an upregulation of both MHCII and CD86 in CX3CR1-ER$^{F/-}$ cells compared to ER$^{F/+}$ cells, indicating increased antigen presentation. Therefore, DNA damage accumulation in microglia leads to a "primed" phenotype, driving innate immune response.

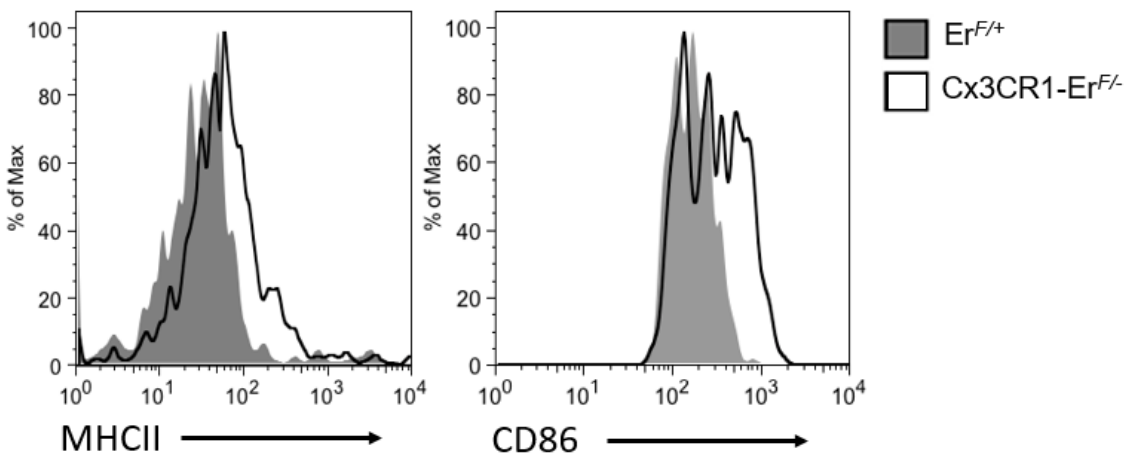

Figure 10: DNA damage accumulation in microglia primes innate immune response. Levels of MHCII and CD86 membrane expression were measured by flow cytometry in CX3CR1-ER$^{F/-}$ (ko) and ER$^{F/+}$ (wt) brains. Higher MHCII/CD86 expression in CX3CR1-ER$^{F/-}$ (ko) brains indicates increased antigen presentation. More mice need to be assessed to reach statistical significance.

3.3 There is no obvious peripheral monocyte infiltration in the brain

According to observed inflammation in CX3CR1-ER$^{F/-}$ cells, we examine the possibility of monocyte peripheral infiltration in the brain. Brain sections from 6-month old CX3CR1-ER$^{F/-}$ (ko) and ER$^{F/+}$ (wt) mice were performed and analyzed by H & E staining. It has been shown that the degree of infiltration (accumulation of cells in spots) assessed by visual evaluation of hematoxylin-eosin (H and E) stained samples. We focused on the cerebellar cortex (CTX) and cerebral cortex (CBX) in due to their involvement in the motor movement regulation. As shown in figure 11A, there is no obvious peripheral monocyte infiltration in CX3CR1-ER$^{F/-}$ tissue sections compared to ER$^{F/+}$ tissue sections. In order to confirm this observation, cells from CX3CR1-ER$^{F/-}$ (ko) and ER$^{F/+}$ (wt) mice were collected and lysed for protein analysis. Western blot analysis was performed to identify the expression or not of CD45 protein, a protein tyrosine phosphatase expressed by all nucleated cells of hemopoietic

lineage. CD45 expression does not appear any difference between CX3CR1-ER$^{F/-}$ (ko) and ER$^{F/+}$ (wt) samples (figure 11B). These results together show, that the observed mice phenotype is orchestrated, at this stage, only by brain resident microglia.

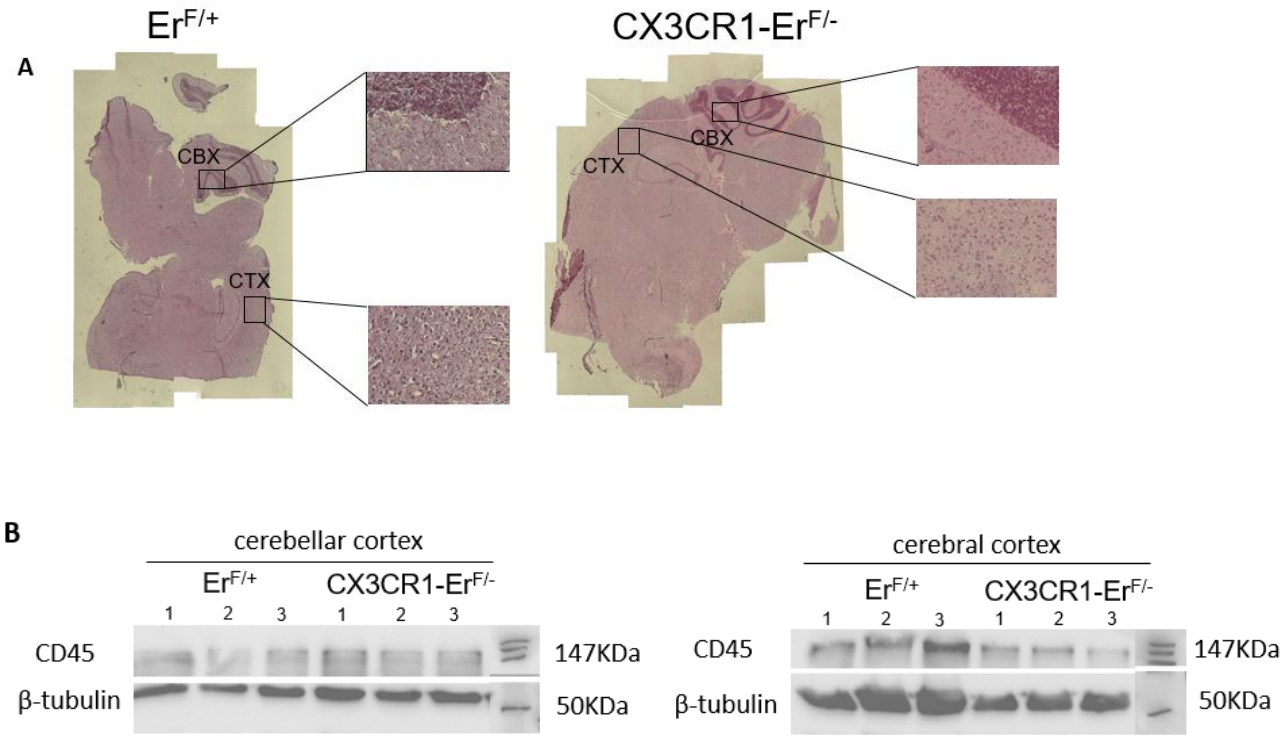

Figure 11: There is no obvious peripheral monocyte infiltration in the brain. (A) Histological analysis of brain sections of 6 months-old CX3CR1-ER$^{F/-}$ (ko) and ER$^{F/+}$ (wt) mice with hematoxylin and eosin staining (karagogeos lab). (B) Western blot analysis for CD45 (marker for myeloid cell origin) protein levels. Mice phenotype is orchestrated by brain resident microglia. More mice need to be assessed to reach statistical significance.

3.4 DNA damage-induced microglia priming leads to Purkinje cell apoptosis

According to our mouse model phenotype, cerebellar ataxia like- neuropathology, it was reasonable to test whether neuronal cell death is occurred, and demyelination is present. In order to examine cell death, we performed TUNEL assay (by Iliana Rouska) in two different brain areas, cerebellar cortex and cerebral cortex, used brain sections from 3- month old and 6-month old CX3CR1-ER$^{F/-}$ (ko) and ER$^{F/+}$ (wt) mice. TUNEL is a method for detecting apoptotic DNA fragmentation, widely used to identify and quantify apoptotic cells. As shown in figure 12A, cell death is observed in CX3CR1-ER$^{F/-}$ (ko) sections (green spots), with increased number of positive cells (apoptotic cells) in the cerebellar cortex (cerebellum) of 6-month old sections, compared to the cerebral cortex. It is worth to notice, that the levels of cell death in 3-month old sections are strongly fewer than 6-month old, with raised apoptosis in the cerebellum (figure 12A). These observations are consistent with the onset of ataxia like symptoms at 4-months old. It is obvious that DNA damage-induced microglia leads to cell death.

To further support this observation, microglia were immune-stained and found also positive for Caspase-3, a crucial mediator for programmed cell death, apoptosis. 6-month old brain sections of cerebellar cortex and cerebral cortex from CX3CR1-ER$^{F/-}$ (ko) and ER$^{F/+}$ (wt) mice were stained against Caspase-3(red)-marker of apoptosis and counterstained with DAPI. As shown in figure 12B, the Caspase-3 expression is highly elevated in the cerebellum of CX3CR1-

$ER^{F/-}$ (ko) mice compared to the cerebral cortex and with $ER^{F/+}$ (wt) mice, respectively. In the cerebellar cortex, Caspase-3 intensity is more intense in a specific area, where normally Purkinje cells, main neuronal population in the cerebellum, are located, providing a first indication that not only neuron cell death is occurred, but also, at this stage of disease, Purkinje cells are more vulnerable to cell death.

In order to confirm the latest observation, we examined the cell death of Purkinje cells with FACs analysis. Therefore, staining with Annexin V was used in conjunction with a vital dye such as propidium iodide (PI) for identification of early and late apoptotic/necrotic cells. Cells that are considered viable are both Annexin V and PI negative, while cells that are in early apoptosis are Annexin V positive and PI negative, and cells that are in late apoptosis or already dead are both Annexin V and PI positive. Meanwhile with Annexin V/PI, Calbindin expression, a specific marker for Purkinje cells was measured by flow cytometry in isolated whole brain samples from CX3CR1-$ER^{F/-}$ (ko) and $ER^{F/+}$ (wt) mice, 8-months old. As shown in figure 12C, 37% of Calbindin+ (Calbindin positive) cells was both Annexin V and PI positive in CX3CR1-$ER^{F/-}$ (ko) mice compare to $ER^{F/+}$ (wt) mice, indicating late apoptosis or already death of Purkinje cells. Consequently, DNA damage-induced microglia priming leads to Purkinje cell apoptosis.

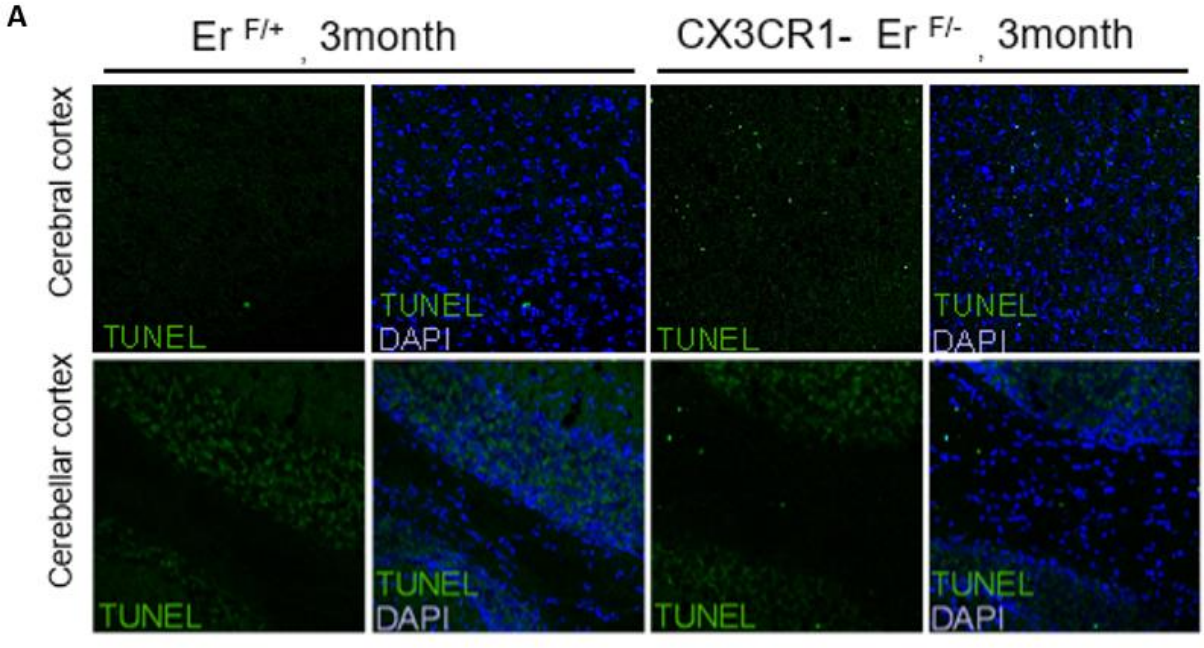

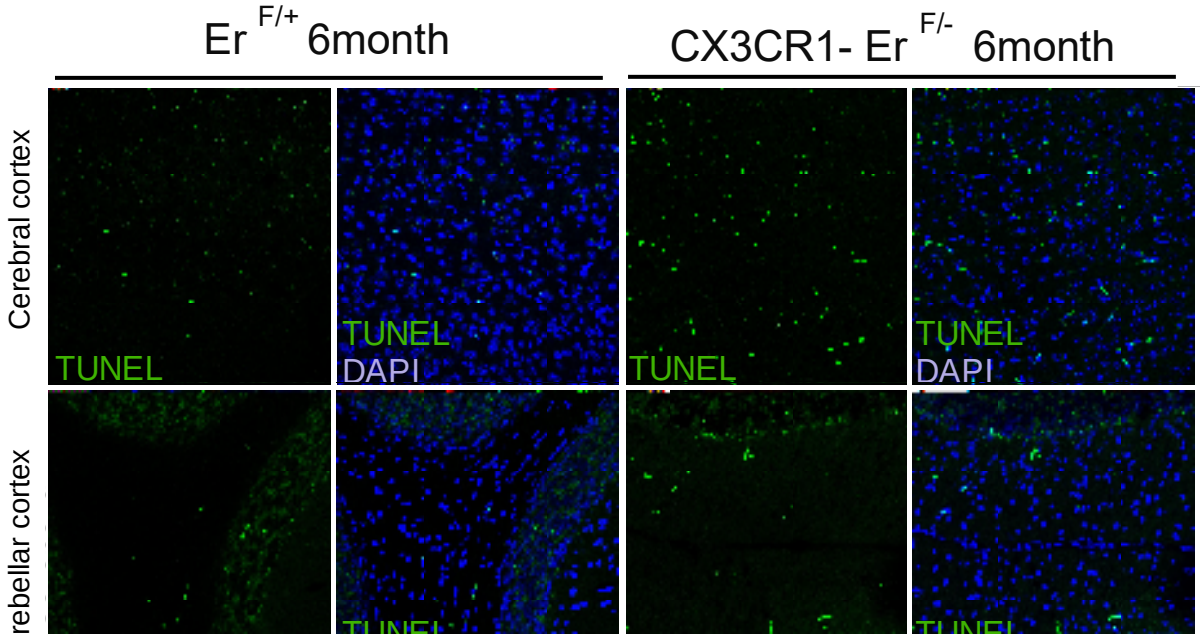

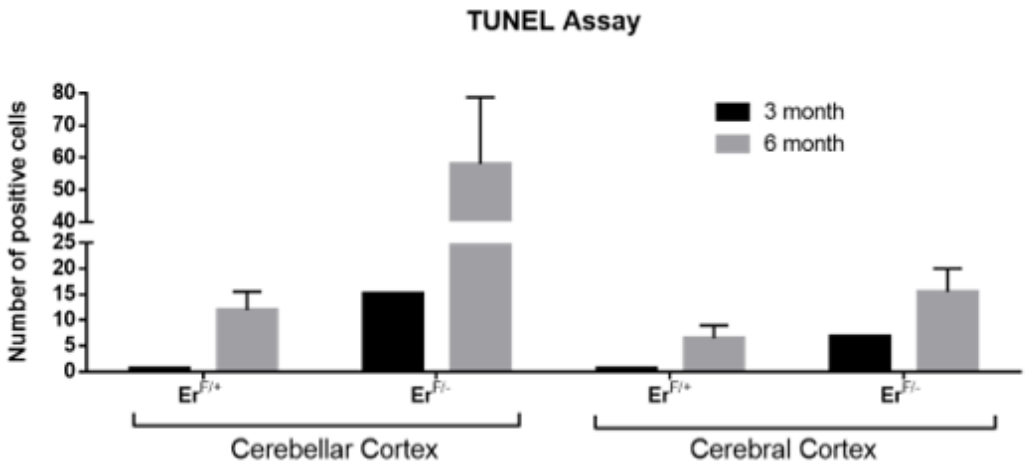

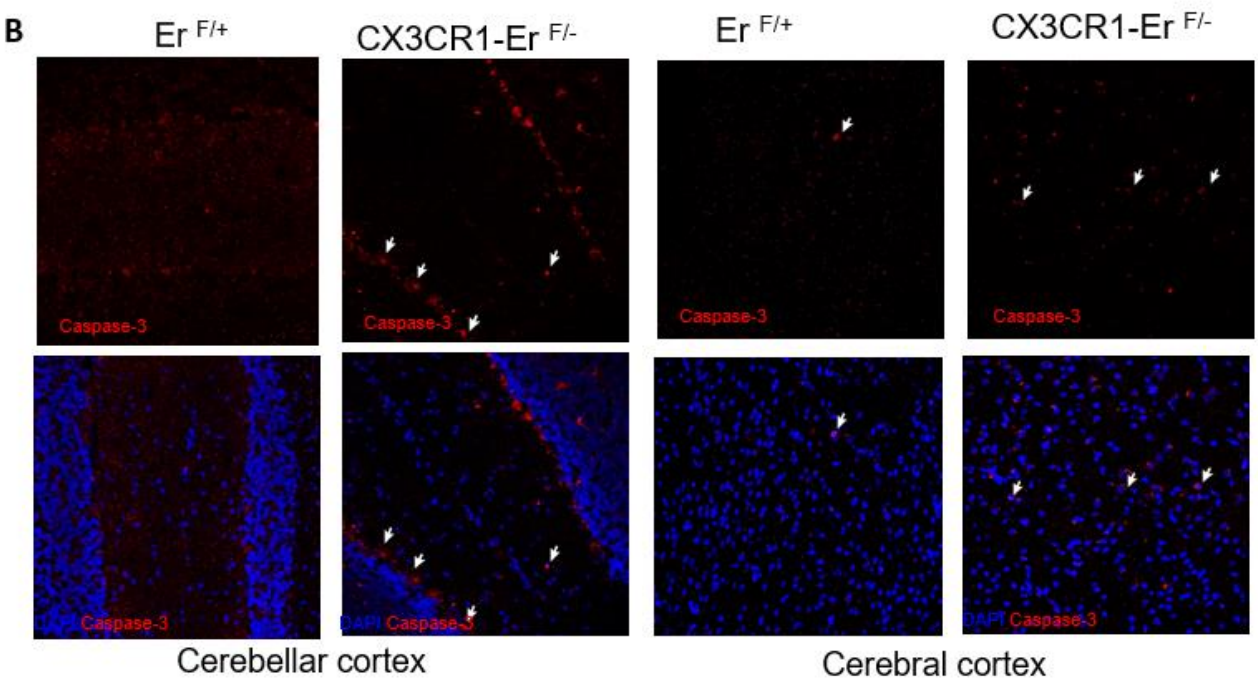

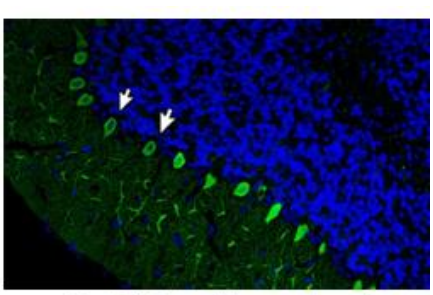

Purkinje cell topology in cerebellar cortex

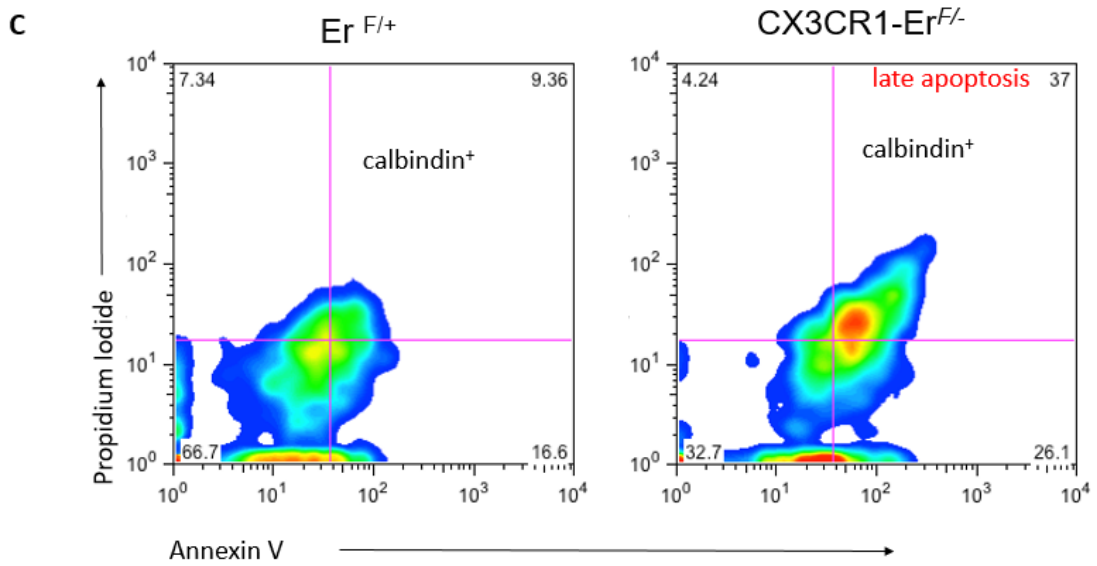

Figure 12: DNA damage-induced microglia priming leads to Purkinje cell apoptosis. Confocal projetions of brain sections of cerebellar cortex and cerebral cortex from 3- month old and 6-month old, CX3CR1-ER$^{F/-}$ (ko) and ER$^{F/+}$ (wt) mice. (A) Tunel assay was performed (green) and sections were counterstained for DAPI (blue). Cell death is increased in the cerebellar cortex of 6-month old CX3CR1-ER$^{F/-}$ (ko) mice. (B) Brain sections were stained for Cleaved Caspase-3- marker for apoptosis and counterstained with DAPI (blue). The Caspase-3 expression is highly elevated in the cerebellum of CX3CR1-ER$^{F/-}$ (ko) mice. (C) Levels of apoptosis in Calbindin positive cells (marker for Purkinje cells) were measured by flow cytometry – Annexin/PI, indicating late apoptosis or already death of Purkinje cells. Magnification x63. More mice need to be assessed to reach statistical significance.

3.5 Dymyelination is not occurred in CX3CR1-ERF/- (ko) mice

Next, we examined if demyelination is occurred. Brain sections from 8-month old CX3CR1-ER$^{F/-}$ (ko) mice compare to ER$^{F/+}$ (wt) mice were stained against Fluoromyelin, fluorescent myelin stain that enables quick and selective labeling of myelin in brain cryosections. As shown in figure 13, there is no obvious difference in the Fluoromyelin intensity between wt and ko mice. However, it is worth noting that more mice need to be assessed to reach statistical significance. (Karagogeos lab)

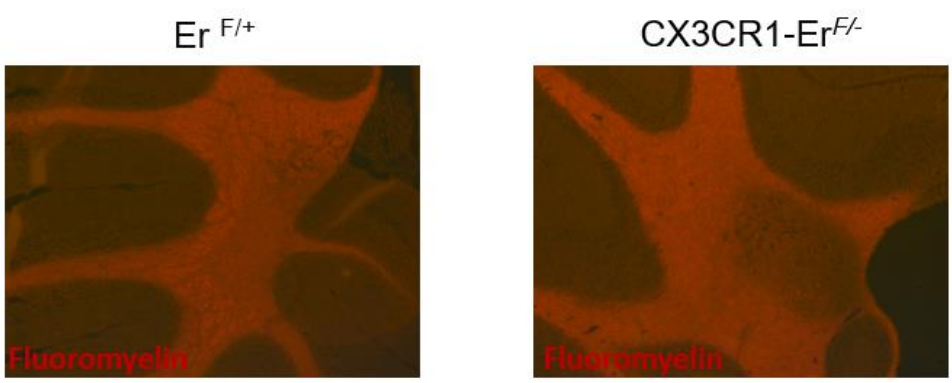

Figure 13 : There is no obvious decrease in myelin in CX3CR1-Er$^{F/-}$ ko mice. Brain cryosections were stained with fluoromyelin (red), fluorescent dye for myelin protein.

Cerebellar cortex is depicted. More mice need to be assessed to reach statistical significance. (karagogeos lab)

3.6 Chromatin fragments accumulation in the cytoplasm of CX3CR1-Er$^{F/-}$ microglia and the role of nucleophagy

As mentioned before, there is a functional interaction between the nucleus and the cytoplasm of CX3CR1-ErF/- microglia. A possible link between these two intracellular compartments is the nuclear autophagy. In order to test whether damaged DNA (γH2Ax signal) and pATM are transported to the cytoplasm through nucleophagy, freshly isolated microglia cells from CX3CR1-ER$^{F/-}$ (ko) and ER$^{F/+}$ (wt) mice were stained with LC3, a marker of autophagy, p62, a selective substrate for autophagy and Mac-1/CD11b, a microglia marker and counterstained with DAPI. As shown in figure 14A, DAPI signal indicating the presence of chromatin fragments is appeared in the cytoplasm of CX3CR1-ER$^{F/-}$ (ko) cells, whereas is absent in the cytoplasm of ER$^{F/+}$ (wt) cells. These chromatin fragments are surrounded by LC3 in ko microglia. Furthermore, cytoplasmic pATM, p62, LC3 and chromatin fragments are co-localized in CX3CR1-ER$^{F/-}$ (ko) microglia cells (figure 14B). All together supports the evidence that the accumulation of chromatin fragments in the cytoplasm is nucleophagy-mediated and pATM dependent.

To further confirm the presence of cytoplasmic DNA (chromatin fragments) in CX3CR1-ER$^{F/-}$ (ko) mice, brain sections from both ko and wild type were stained against MAC-1/ CD11b (microglia marker) and dsDNA and counterstained with DAPI. To avoid the possibility the dsDNA antibody stains nuclear DNA, we used a permeabilization reagent, called digitonin, which does not disrupt the nuclear membrane. As shown in figure 14C, cytoplasmic double-stranded DNA accumulates in CX3CR1-ER$^{F/-}$ (ko) brain areas enriched in microglia, whereas this is not observed in ER$^{F/+}$ (wt) brain areas. It is now clear that unrepaired DNA damage in CX3CR1-ER$^{F/-}$ (ko) microglia triggers accumulation of cytoplasmic dsDNA (chromatin fragments).

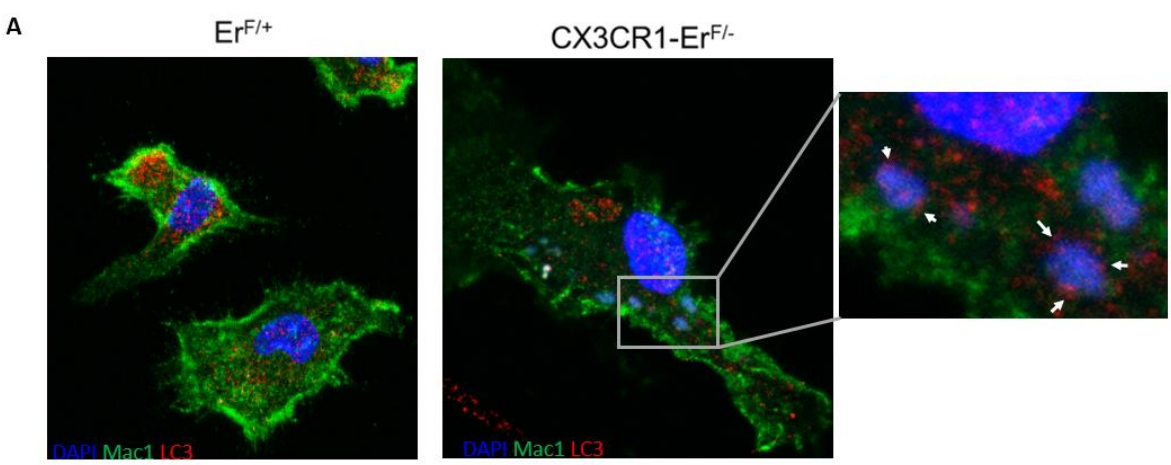

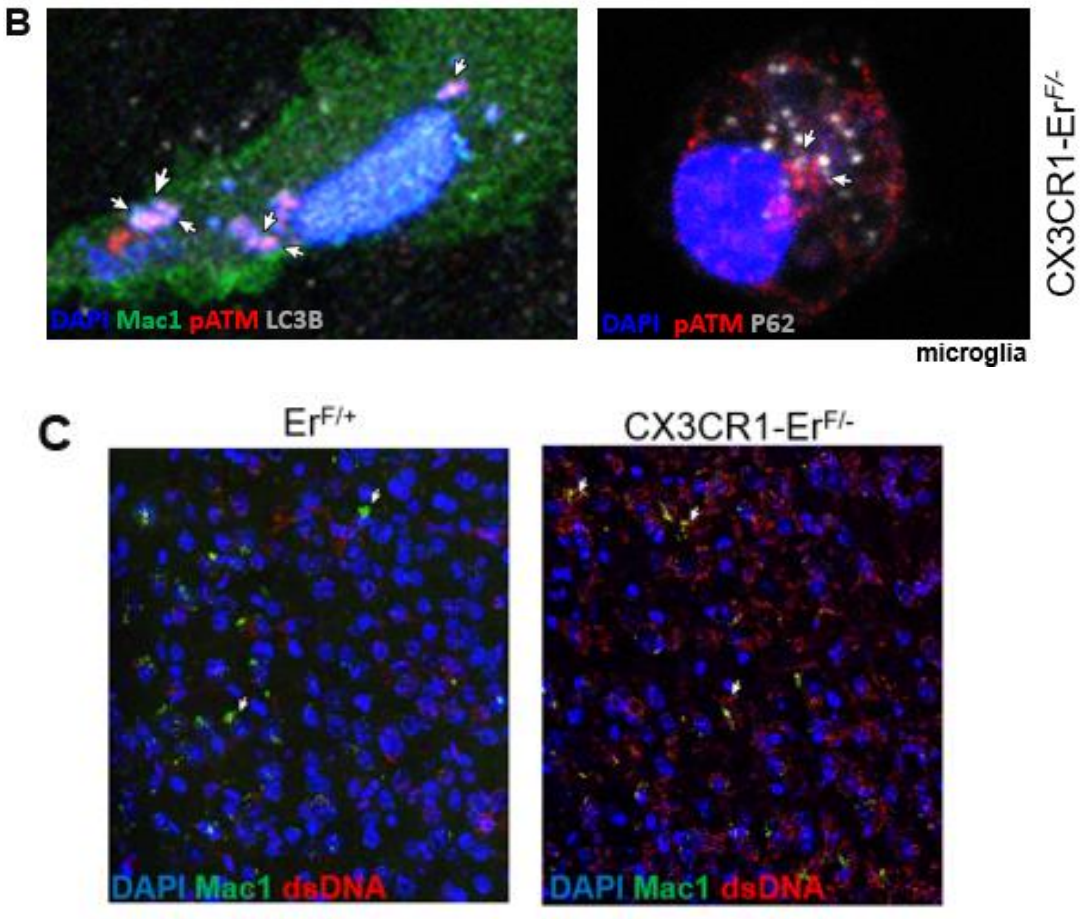

Figure 14: Chromatin fragments accumulation in the cytoplasm of CX3CR1-Er$^{F/-}$ microglia and the role of nucleophagy. (A,B) Confocal projetions of microglia cells from CX3CR1-ER$^{F/-}$ (ko) and ER$^{F/+}$ (wt) mice were stained for (A) Mac1-microglia marker (green), LC3B- autophagy protein (red), (B) Mac1-microglia marker (green), LC3B- autophagy protein (white), pATM- DNA damage marker (red) and p62- selective substrate for autophagy (white) and counterstained with DAPI (blue). Chromatin fragments in the cytoplasm of CX3CR1-ER$^{F/-}$ (ko) cells are surrounded by LC3B and co-localized with pATM and p62. (C) Brain tissue sections from CX3CR1-ER$^{F/-}$ (ko) and ER$^{F/+}$ (wt) mice were stained for Mac1-microglia marker (green), dsDNA antibody (red) and counterstained with DAPI (blue). Cytoplasmic dsDNA accumulates in CX3CR1-ErF/- brain areas enriched in microglia. Magnification x63. More mice need to be assessed to reach statistical significance.

3.7 STING sensing and type I IFN response is activated in CX3CR1-ErF/- brain

According to the bibliography, the presence of cytoplasmic DNA sensed by specific DNA sensors located in the cytoplasm, inducing an immune response and robustly type I IFN signaling. In order to examine whether type I IFN signaling is activated, we assessed the protein levels of STING, a known interferon response gene (ISG). To this end, cells from CX3CR1-ER$^{F/-}$ (ko) mice and ER$^{F/+}$ (wt) mice were collected and lysed for protein analysis. As shown in figure 15A, there is a trend for increased STING levels in ko cerebellum compared to wild type, suggesting type I IFN signaling activation upon persistent DNA damage. However, it is worth noting that more mice need to be assessed to reach statistical significance.

According to this observation, we next examined type I IFN signaling activation by measured the mRNA levels of IFNa, IFNβ as well as, specific type I IFN stimulated-genes (ISGs), such as IFIT2, MX1, IRF1 and IFI207. Whole brains from CX3CR1-ER$^{F/-}$ (ko) mice and ER$^{F/+}$ (wt) mice were isolated and lysed for mRNA analysis by qPCR. As shown in figure 15B, the mRNA levels of these genes are highly elevated in CX3CR1-ER$^{F/-}$ (ko) brains compared to ER$^{F/+}$ (wt) ones, suggesting the type I IFN signaling activation in CX3CR1-ER$^{F/-}$ (ko) mice.

To further confirm the last observation, we used a reporter cell line to identify type I IFN response. B16-Blue IFN α/β cells were cultured and treated with an amount of different culture media deriving from microglia cells. Their supernatants were collected and used in a reporter assay, that determines the secretion of IFN-α and IFN-β. In more detail, B16-Blue IFN-α/β cells allow the detection of bioactive murine type I IFNs, by monitoring the activation of the JAK/STAT/ISGF3 pathway. In figure 15C , we show that microglia secreted IFN-α/β activity was higher in CX3CR1-ER$^{F/-}$ (ko) mice compared to the ER$^{F/+}$ (wt) mice, thus indicating that the type I IFN response is highly activated in ko mice. Taken all together, accumulation of cytoplasmic dsDNA triggers the type I IFN response through STING pathway in CX3CR1-ER$^{F/-}$ (ko) mice.

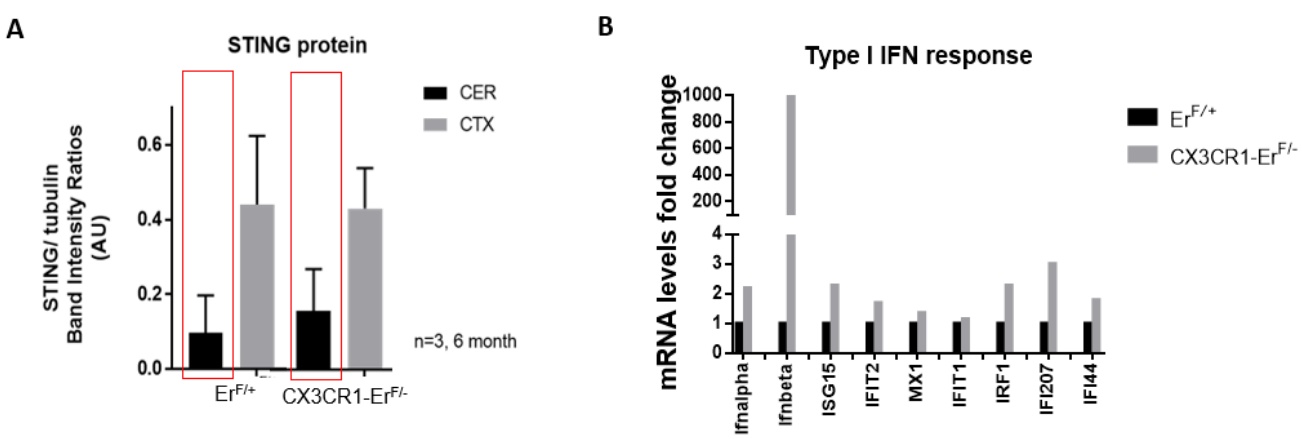

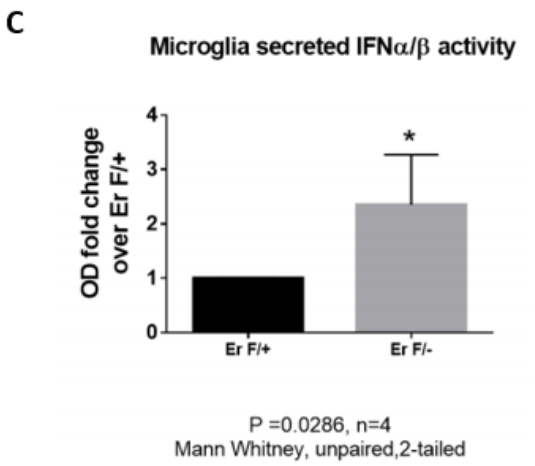

Figure 15: STING sensing and type I IFN response is activated in CX3CR1-ErF/- brain. (A) Western blot analysis for STING (a known interferon response gene) protein levels in the cerebellar cortex and cerebral cortex of CX3CR1-ER$^{F/-}$ (ko) and ER$^{F/+}$ (wt) brains. There is a trend for increased STING levels in ko cerebellar cortex. (B) Relative mRNA expression of ISGs (interferon response genes) compared to HPRT in CX3CR1-ER$^{F/-}$ (ko) and ER$^{F/+}$ (wt) brains. Type I IFN response is activated in ko brains. More mice need to be assessed to reach statistical significance (A, B). (C) Reporter assay of B16-Blue IFN α/β cells with microglia cells culture media. Microglia secreted IFN-α/β activity is significantly higher in ko mice compared to the wt ones. Mann Whitney U test.

3.8 IFNAR+ Purkinje cells die through apoptosis in CX3CR1-Er$^{F/-}$ brain

Until now, we have shown that Purkinje cells die with apoptosis and that type I interferone response is activated in CX3CR1-Er$^{F/-}$ mice. According to these data, we asked whether there is a link between two phenomena. For this reason, Calbindin expression, a specific marker for Purkinje cells and IFNAR expression, interferon-alpha/beta receptor was measured by flow cytometry in isolated whole brain samples from CX3CR1-ER$^{F/-}$ (ko) and ER$^{F/+}$ (wt) mice, 8-months old. In CX3CR1-ER$^{F/-}$ (ko) brain, 45.3% of Purkinje cells (Calbindin positive) expresses IFNAR compared to 35.6% in ER$^{F/+}$ (wt) brain (figure 16A). Also, the mean fluorescent intensity of IFNAR molecules per Purkinje cell is higher in ko brain (96.2) than the number of IFNAR molecules in wt brain, suggesting that Purkinje cells in CX3CR1-ER$^{F/-}$ (ko) mice are more vulnerable to type I IFN response (figure 16A).

Furthermore, it remains to be assessed if type I IFN response is responsible for Purkinje cell death. To this end, staining with Annexin V was used in conjunction with a vital dye such as propidium iodide (PI) for identification of early and late apoptotic/necrotic cells by flow cytometry. In parallel with this, we observed the expression of Calbindin and IFNAR in CX3CR1-ER$^{F/-}$ (ko) brains. As shown in figure 16B, from all the IFNAR+ cells in CX3CR1-ErF/- brain, only Purkinje cells die with late apoptosis. All data together suggest that in CX3CR1-ErF/- brain, IFNAR+ Purkinje cells die through apoptosis.

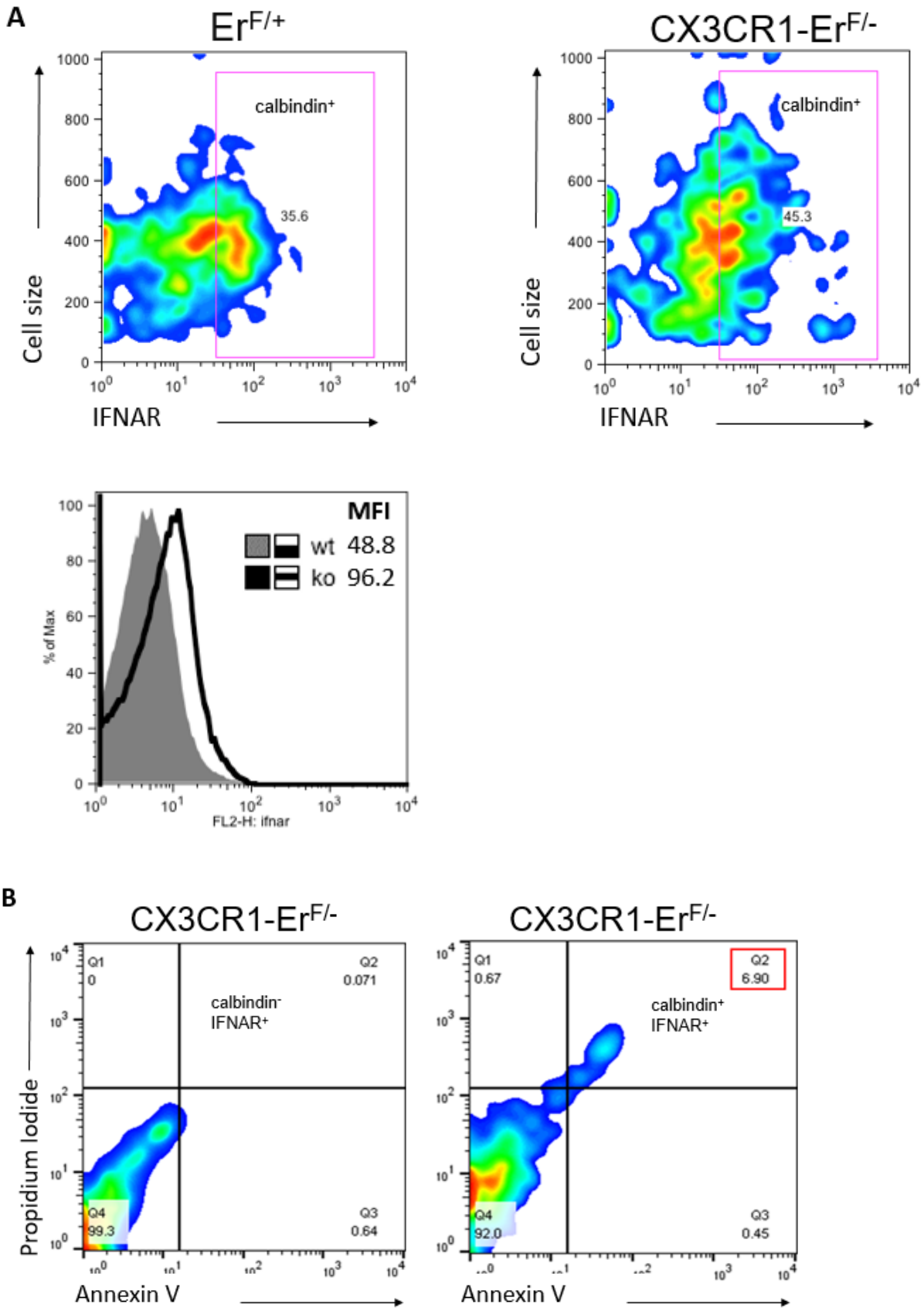

Figure 16: IFNAR+ Purkinje cells die through apoptosis in CX3CR1-Er$^{F/-}$ brain. (A) Levels of IFNAR (IFNα/β receptor) membrane expression in Calbindin positive cells (Purkinje cells) were measured by flow cytometry. Mean fluorescence intensity (MFI) averages are plotted.

Purkinje cells receive Type I IFN signaling in CX3CR1-ErF/- mice. (B) Levels of apoptosis in IFNAR positive cells and Calbindin levels were measured by flow cytometry – Annexin/PI, indicating that out of all the IFNAR+ cells in CX3CR1-ErF/- brain, only Purkinje cells die with late apoptosis. More mice need to be assessed to reach statistical significance.

3.9 DNA damage accumulation in microglia enhances the secretion of dsDNA loaded, Mac1+ (CD11b) exosomes

According to our data, chromatin fragments are accumulated in the cytoplasm of CX3CR1-ErF/- microglia and are sensed by DNA sensors triggering immune response. Now, it makes sense to ask what the fate of these cytoplasmic chromatin fragments is. We examined the possibility of chromatin fragments release in the extracellular space. Consistent with this, we performed FACs analysis to check the granularity status of microglia cells (CD11b/Mac1 marker) in CX3CR1-$ER^{F/-}$ (ko) brains and $ER^{F/+}$ (wt) brains. We observed high vesicle content in CX3CR1-$Er^{F/-}$ microglia, suggesting the presence of vesicles intracellularly (figure 17A). To further assess if these vesicles are secreted to the extracellular space, we isolated intact exosomes (according to an established protocol for exosome isolation) from the milieu of CX3CR1-$ER^{F/-}$ (ko) brains and $ER^{F/+}$ (wt) brains. Western blot analysis showed an enrichment of exosome specific markers, CD9, CD81 and ALIX, that are involved in the biogenesis, targeting, transport and function of exosomes. In addition, with exosome specific markers, in CX3CR1-$ER^{F/-}$ (ko) samples, there is an increase in p62 expression, compared to wt ones (this protein was co-localized with chromatin fragments) (figure 17B). To confirm this observation, TEM (transmission electron microscopy) and SEM (scanning electron microscopy) is used. As shown in figure 17C and D, electron microscopy reveals the presence of exosomes in media of CX3CR1-$ER^{F/-}$ (ko) brains with a size ranging between 30-100nm (that corresponds to bibliography). Therefore, DNA damage accumulation triggers the release of exosomes from CX3CR1-$ER^{F/-}$ (ko) brains.

In order to identify the cell origin of secreted exosomes and the exosome cargo, we performed FACs analysis. CD11b/Mac1, a microglia marker, expression in exosomes isolated from the media of CX3CR1-$ER^{F/-}$ (ko) brains and $ER^{F/+}$ (wt) brains, was measured by flow cytometry. Also, exosomes were stained with picogreen, an ultra-sensitive fluorescent nucleic acid stain for quantitating double-stranded DNA (dsDNA). As shown in figure 17E, from the CD11b positive exosomes (microglia cell origin), picogreen expression is enhanced in CX3CR1-$ER^{F/-}$ (ko) ones. Consequently, DNA damage accumulation in microglia enhances the secretion of dsDNA loaded, CD11b/Mac1 positive exosomes.

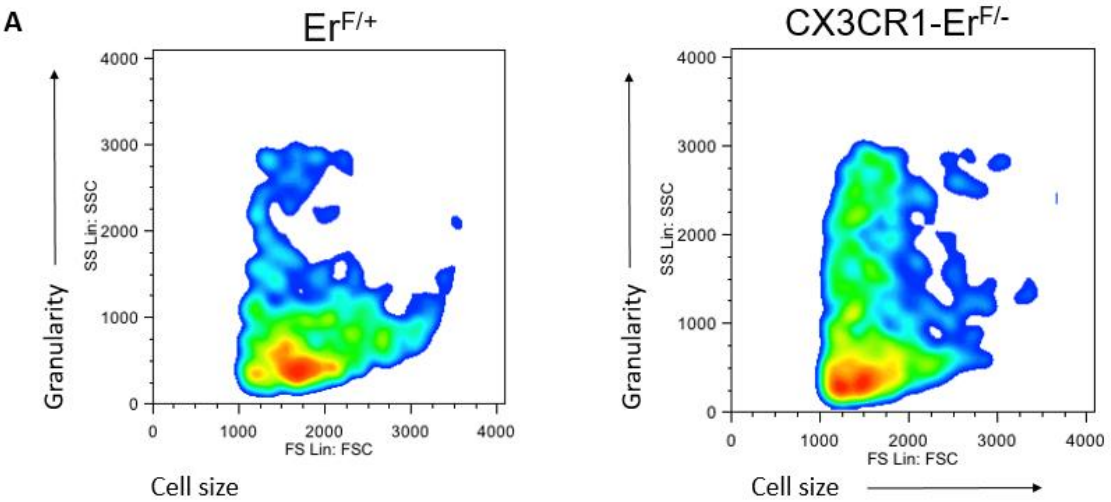
A
Er^F/+
CX3CR1-Er^F/-
Granularity
SS Lin: SSC
FS Lin: FSC
Cell size
0
1000
2000
3000
4000

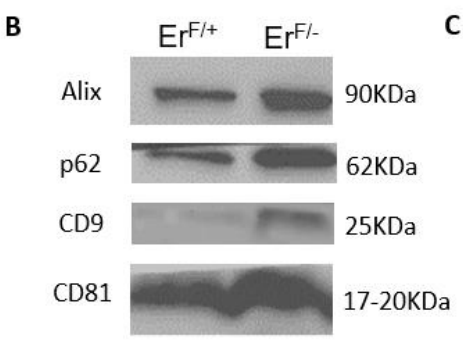
B
Er^F/+
Er^F/-
Alix
90KDa
p62
62KDa
CD9
25KDa
CD81
17-20KDa

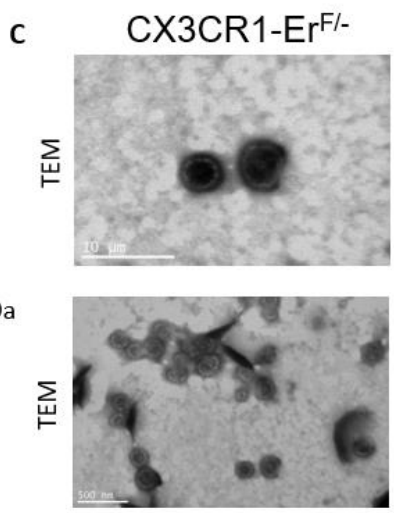
C
CX3CR1-Er^F/-
TEM
TEM

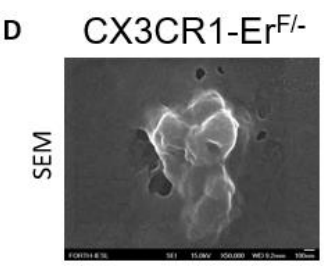
D
CX3CR1-Er^F/-
SEM

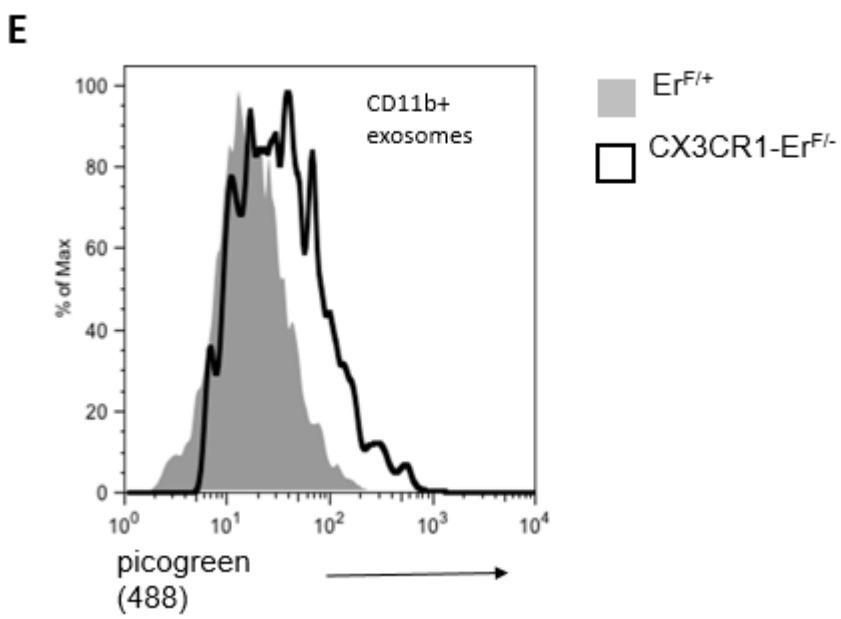
E
CD11b+
exosomes
Er^F/+
CX3CR1-Er^F/-
% of Max
picogreen
(488)

Figure 17: DNA damage accumulation in microglia enhances the secretion of dsDNA loaded, Mac1+ (CD11b) exosomes. (A) The granularity status of microglia cells (CD11b/Mac1 marker) in CX3CR1-ER$^{F/-}$ (ko) brains and ER$^{F/+}$ (wt) brains was analyzed by flow cytometry, indicating the presence of high vesicle content in ko brains. (B) Western blot analysis for exosomal proteins levels in exosomes isolated from CX3CR1-ER$^{F/-}$ (ko) brains and ER$^{F/+}$ (wt) brains. Enrichment of these proteins in ko brains. (C, D) TEM and SEM analysis of exosomes isolated from CX3CR1-ER$^{F/-}$ (ko) brains. (E) DNA content (picogreen dye) was checked by flow cytometry in CD11b positive exosomes. Picogreen expression is enhanced in CX3CR1-ER$^{F/-}$ (ko) ones.

3.10 Decreased levels of IFNα/β in CX3CR1-ERF/- (ko) mice treated with DNaseI-loaded exosomes.

In an effort for further support the causative correlation between the presence of cytoplasmic chromatin fragments and the activation of type I IFN response, we used exosomes as a tool. In more details, we used naïve exosomes and exosomes with recombinant DNaseI. Freshly isolated microglia cells from CX3CR1-ER$^{F/-}$ (ko) mice were treated with naïve exosomes and DNaseI-loaded exosomes. The medium of these cells had kept, added to a reporter cell line, B16-Blue IFN α/β cells, to identify type I IFN response. In figure 18, we show that microglia secreted IFN-α/β activity decreased with DNaseI-loaded exosomes treatment compared to naïve exosomes treatment. This result shows that decreased levels of IFNα/β are found in CX3CR1-ERF/- (ko) mice treated with DNaseI-loaded exosomes.

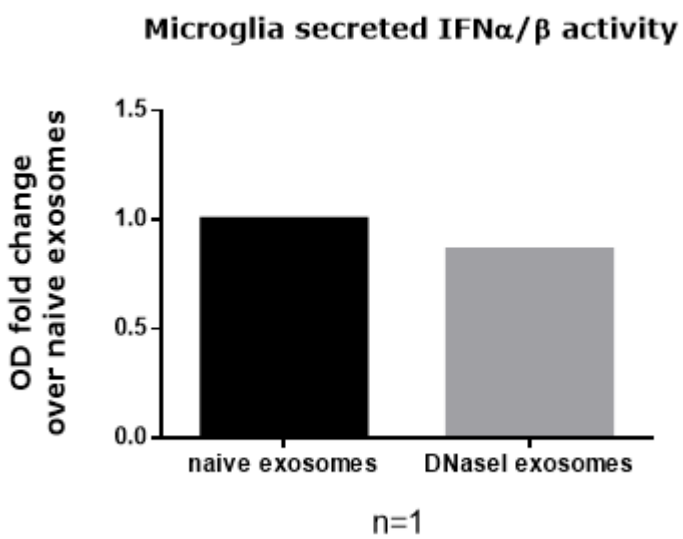

Figure 18: Decreased levels of IFNα/β in CX3CR1-ERF/- (ko) mice treated with DNaseI-loaded exosomes. Reporter assay of B16-Blue IFN α/β cells with microglia cells (from CX3CR1-ER$^{F/-}$ (ko) mice) culture media treated with naïve exosomes and DNaseI exosomes. Microglia secreted IFN-α/β activity is higher in cells treated with DNaseI exosomes. More mice need to be assessed to reach statistical significance

3.11 Immunolabeling of mouse acute brain slices- protocol standardization

In order to examine the role of these extracellular vesicles and the Purkinje cells vulnerability, we decided to check exosome uptake by Purkinje cells. Acute brain slices protocol was used for this purpose. Acute brain slices are widely used for electrophysiological experiments and live imaging using two-photon laser scanning microscopy, which allows for visualization of cells deep within the tissue. They provide the convenience of cultured cells in terms of timely pharmacological interventions and easy manipulations (e.g., accessibility of electrodes), while preserving the cyto-architecture and natural cell-cell interactions of the brain region of interest. Although immunolabeling is routinely used to visualize target proteins in cultured cells and in thin cryostat sections of brains fixed by transcardial perfusion, it is not commonly used for acute brain slices. One reason is because the optimal thickness for acute brain slices is between 300 and 400 µm, which compromises the penetration of both fixatives and antibodies. Consequently, it becomes problematic to fix fine structures within the tissue, and subsequent immunolabeling of target proteins requires cryostat resectioning. Thus, SNAPSHOT method was established. This method is said to allow the rapid fixation and immunolabeling of target proteins within thick brain slices. In order to determine if this method was in fact valid, we used acute brain slices of a wt mouse, which we then fixated and immunolabeled with Mitotracker and Picogreen, a cytoplasmic (mitochondrial stain) and a dsDNA marker, respectively. The results were satisfying, as shown in figure 19, since both antibodies were able to successfully penetrate through the thick tissue and the tissue's depth is also visible.

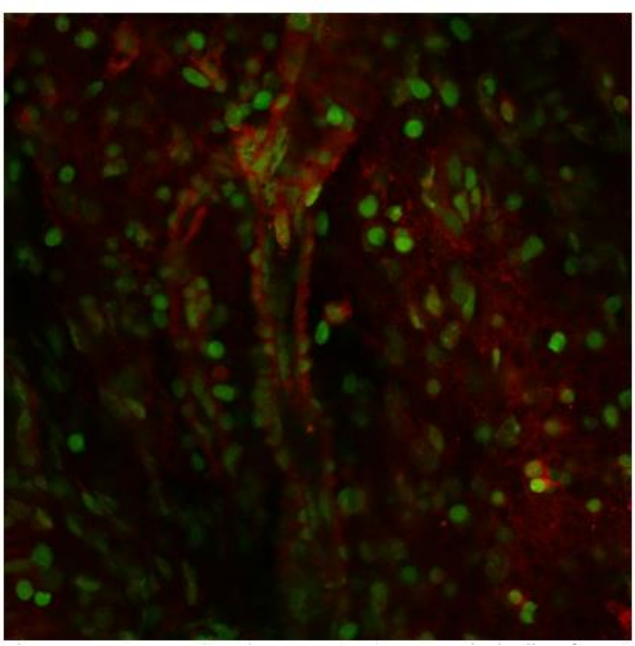

Figure 19: Immunolabeling of mouse acute brain slices. Acute brain slices from a wt mouse were fixated and successfully immunolabeled with Mitotracker (red) and Picogreen (green). Mitotracker is a cytoplasmic marker and Picogreen is a nuclear marker.

Chapter IV:

Discussion

In this study we used a monocyte/macrophage-specific Ercc1-/- mouse (Cx3cr1-Cre) to impair DNA repair in tissue resident macrophages. According to our mouse phenotype, cerebellar ataxia neuropathology, we focused our research in brain (and spinal cord, in general CNS) resident macrophages, called microglia cells. Microglia promote phagocytic clearance, provide trophic support to ensure tissue repair, protect neurons and maintain brain homeostasis. Alterations in microglia functionality are implicated in brain development and aging, as well as in neurodegeneration. In accordance to that, we examined whether microglia- specific DNA damage accumulation is enough to drive age- related neuropathology and we obtained some indications about it.

Firstly, we confirmed the functionality of the Cx3CR1 KO model. Ercc1 deletion in microglia triggers sustained DNA Damage Response (DDR) and accumulation of DNA damage, indicating by the increased presence of DNA damage specific markers (γH2Ax and pATM) in the nucleus. Surprisingly, we observed also cytoplasmic accumulation of these markers in CX3CR1-ER$^{F/-}$ (ko) microglia cells. The functional role of this presence in the cytoplasm will be discussed below. Secondly, we observed the highly ramified morphology of microglia cells in CX3CR1-ER$^{F/-}$ (ko) mice, which is consistent with its cell identity as antigen presenting cell. After that, we asked whether the morphological change is accompanied with a change in microglial activation. We actually found out that CX3CR1-ER$^{F/-}$ (ko) microglia cells show increased antigen presentation and related to aforementioned literature, microglia phenotype is characterized as primed (Holtman et al., 2015). Primed microglia are characterized by an exaggerated and uncontrolled inflammatory response to an immune stimulus. Therefore, microglia in CX3CR1-ER$^{F/-}$ (ko) mice prime innate immune activation. After histological analysis of brain areas, we observed no obvious infiltration by peripheral monocytes, indicating that only brain resident macrophages, microglia, are responsible for the characterized mouse phenotype, at least at the age stage we study.

As mentioned before, there is a functional interaction between the nucleus and the cytoplasm of CX3CR1-ErF/- microglia. We hypothesized that nucleophagy could be a key mediator in this process. Chromatin fragments were accumulated in the cytoplasm of CX3CR1-ER$^{F/-}$ (ko) microglia cells. These chromatin fragments were surrounded by LC3 and co-localized with pATM and p62. LC3 and p62 are major proteins involved in autophagy. In accordance to the literature, there are a lot of cases that genomic DNA, in the form of chromatin, escape from the nucleus into the cytoplasm. Nuclear DNA damage can cause the formation of micronuclei, abnormal nuclear structures. Micronuclei (are stained positive for γH2AX, a DNA damage marker) are surrounded by nuclear envelope and a small portion of observed micronuclei are surrounded by double membrane vesicles and are stained positive for autophagosomal and lysosomal markers, indicating the autophagy involvement in sequestration and degradation. Furthermore, nuclear materials, such as chromatin fragments, are encapsulated by the nuclear membrane in response to the interaction of two proteins, LaminB1 and LC3. In senescent cells, nuclear membrane autophagosomes/vesicles containing chromatin fragments (stained positive for γH2AX and heterochromatin markers) eventually partition into the cytoplasm to become cytoplasmic chromatin fragments (Harding et al., 2017; Rello-Varona et al., 2012).

The chromatin fragments which are present in the cytoplasm of CX3CR1-ER$^{F/-}$ (ko) microglia cells, trigger innate immune response through STING sensing and type I IFN response activation. There are numerous recent studies highlighting how genomic DNA serves as a reservoir to initiate a pro-inflammatory pathway in the cytoplasm. Cytosolic DNA (double-stranded DNA) can bind to cGAS which in turn converts GTP into a second messenger cGAMP that binds to STING. STING activation leads to IFN-α/β and proinflammatory cytokines production (Li et al., 2018). Since the cytoplasmic DNA is processed by autophagy/lysosomal pathway, it is not clearly understood how DNA can be sensed by cytoplasmic DNA sensors. Impairment of the autophagy/lysosomal machinery may result in increased presence of DNA in the cytoplasm witch, in turn activates innate immune responses (Lan et al., 2018). In order to assess the role of nucleophagy in microglia cells, we will treat cells with reagents which inhibit nucleophagy and induce lysosomal degradation.

Additionally, it was necessary to monitor the fate of these cytoplasmic chromatin fragments in the brain of CX3CR1-ER$^{F/-}$ (ko) mice. DNA damage accumulation triggers the release of exosomes from CX3CR1-ER$^{F/-}$ (ko) brains. These exosomes are microglia derived and dsDNA loaded. This is a first indication that the chromatin fragments are the cargo of exosomes. To further confirm this, we will immunogold label exosome slices for damaged chromatin. Exosomes are important to transport signals between cells mediating a novel mechanism of cell-to-cell communication in the healthy and diseased brain (Gurunathan et al., 2019). Several studies reveal the role of exosomes in brain cells communication, such as neuron-neuron interactions and glia (microglia, astrocytes and oligodendrocytes)- neuron interactions (Budnik et al., 2016). Neuroinflammation is mediated by the secretion of microglia derived exosomes containing pro- inflammatory factors. There is a constant interplay between exosomes and autophagy. Autophagosomes can fuse with MVBs, creating a hybrid vesicle, called amphisome (Xu et al., 2018). Amphisomes have the ability either to fuse with lysosomes for cargo degradation or fuse with the plasma membrane for secretion of their content. As mentioned before, it is possible there are deficiencies in autophagy/ lysosomal machinery, leading to the sensing of chromatin fragments by cytoplasmic DNA sensors and probably to the loading of these in exosomes. If this hypothesis is not correct, autophagosomes could fuse with MVBs and transfer their content to MVBs, creating amphisomes with subsequently fusion with the plasma membrane and release of exosomes in the extracellular space.

According to the neurological mouse phenotype, we examined neuronal cell death and demyelination. Purkinje cells, neuronal cells located in the cerebellum, die through apoptosis in CX3CR1-ER$^{F/-}$ (ko) mice whereas there is no obvious decrease in myelin abundance in the cerebellum of these ko mice. Purkinje cells receive more type I IFN signaling in CX3CR1-ER$^{F/-}$ (ko) mice. It is worth to notice that, from all the cells in ko brain receiving this signaling, the only ones die with apoptosis are Purkinje cells. Obviously, Purkinje cells are more vulnerable to type I IFN signaling originating from the microglia. Type I IFNs interfere with viral replication and prepare receiving cells to sense the presence of cytoplasmic nucleic acids. When type I IFN signaling is ON and there is presence of exogenous nucleic acids cells die with apoptosis to eliminate “viral” replication yield in the host (Teijaro., 2016). Studies have shown that microglia in the cerebellum are constantly close to Purkinje cells and make dynamic contacts with neuron dendrites and somas. Microglial cell somas were interspersed between the Purkinje neuron somas (Stowell et al., 2018). In this spectrum, it would be possible Purkinje cells are the recipient cells for the microglia derived exosomes. If this is true, the response of Purkinje cells in IFNα/β, as well as exosomal uptake, acting as exogenous nucleic acid, may trigger neuronal cell death by apoptosis. In order to clarify this, we will use acute brain slices. Brain slices will be incubated with fluorescently pre-stained exosomes with or without rIFNα

(recombinant IFNα) and subsequently we will check the exosome uptake and the apoptosis in different brain areas and cell types, using 2- photon analysis. Finally, if the combination of type I IFN signaling and exosomal uptake is responsible for Purkinje cell death, we will try to rescue the phenotype. For this purpose, we will use Mac1-ligand decorated, DNase1 carrying exosomes (potential in therapeutic manipulation) with or without IFNAR blocking antibody and we will observe Purkinje cell death.

Chapter V:

References

Abdulrahman, Basant A., Dalia H. Abdelaziz, and Hermann M. Schatzl. 2018. "Autophagy Regulates Exosomal Release of Prions in Neuronal Cells." Journal of Biological Chemistry 293(23): 8956–68.

Adam Moser, Kevin Range, and Darrin M. York. 2008. "基因的改变NIH Public Access." Bone 23(1): 1–7.

Adams, Peter D. et al. 2013. "Lysosome-Mediated Processing of Chromatin in Senescence." Journal of Cell Biology 202(1): 129–43.

Ahmad, A. et al. 2008. "ERCC1-XPF Endonuclease Facilitates DNA Double-Strand Break Repair." Molecular and Cellular Biology 28(16): 5082–92.

Alegre, Maria Luisa, Kenneth A. Frauwirth, and Craig B. Thompson. 2001. "T-Cell Regulation by CD28 and CTLA-4." Nature Reviews Immunology 1(3): 220–28.

Bai, Juli, and Feng Liu. 2019. "The CGAS-CGAMP-STING Pathway: A Molecular Link between Immunity and Metabolism." Diabetes 68(6): 1099–1108.

Baixauli, Francesc, Carlos López-Otín, and Maria Mittelbrunn. 2014. "Exosomes and Autophagy: Coordinated Mechanisms for the Maintenance of Cellular Fitness." Frontiers in Immunology 5(AUG): 1–6.

Bohr, Vilhelm A. 2018. "DNA Damage, DNA Repair, Aging, and Neurodegeneration."

Brown, Amanda M. et al. 2019. "Molecular Layer Interneurons Shape the Spike Activity of Cerebellar Purkinje Cells." Scientific Reports 9(1): 1–19. http://dx.doi.org/10.1038/s41598-018-38264-1.

Budnik, Vivian, Catalina Ruiz-Cañada, and Franz Wendler. 2016. "Extracellular Vesicles Round off Communication in the Nervous System." Nature Reviews Neuroscience 17(3): 160–72.

Burgess, Matthew, Kate Wicks, Marina Gardasevic, and Kimberly A. Mace. 2019. "Cx3CR1 Expression Identifies Distinct Macrophage Populations That Contribute Differentially to Inflammation and Repair." ImmunoHorizons 3(7): 262–73.

Chatterjee, Nimrat, and Graham C. Walker. 2017. "Mechanisms of DNA Damage, Repair, and Mutagenesis." Environmental and Molecular Mutagenesis 58(5): 235–63.

Chatzinikolaou, Georgia, Ismene Karakasilioti, and George A. Garinis. 2014. "DNA Damage and Innate Immunity: Links and Trade-Offs." Trends in Immunology 35(9): 429–35.

Chen, Jian Hua, C. Nicholes Hales, and Susan E. Ozanne. 2007. "DNA Damage, Cellular Senescence and Organismal Ageing: Causal or Correlative?" Nucleic Acids Research 35(22): 7417–28.

Chen, Wei Wei, Xia Zhang, and Wen Juan Huang. 2016. "Role of Neuroinflammation in Neurodegenerative Diseases (Review)." Molecular Medicine Reports 13(4): 3391–96.

Chow, Hei Man, and Karl Herrup. 2015. “Genomic Integrity and the Ageing Brain.” Nature Reviews Neuroscience 16(11): 672–84. http://dx.doi.org/10.1038/nrn4020.

CNT. 2007. “Stormwater Management, Green Infrastructure, and the Center for Neighborhood Technology.” 13(11): 1118–28.

Crow, Yanick J., and Nicolas Manel. 2015. “Aicardi-Goutières Syndrome and the Type I Interferonopathies.” Nature Reviews Immunology 15(7): 429–40. http://dx.doi.org/10.1038/nri3850.

De Boer, Jan, and Jan H.J. Hoeijmakers. 2000. “Nucleotide Excision Repair and Human Syndromes.” Carcinogenesis 21(3): 453–60.

Derecki, Noël C., James C. Cronk, and Jonathan Kipnis. 2013. “The Role of Microglia in Brain Maintenance: Implications for Rett Syndrome.” Trends in Immunology 34(3): 144–50.

Domeier, Phillip P. et al. 2018. “B-Cell-Intrinsic Type 1 Interferon Signaling Is Crucial for Loss of Tolerance and the Development of Autoreactive B Cells.” Cell Reports 24(2): 406–18. https://doi.org/10.1016/j.celrep.2018.06.046.

Dou, Zhixun et al. 2018. “Cancer.” 550(7676): 402–6.

Dou, Zhixun et al. 2015. “Autophagy Mediates Degradation of Nuclear Lamina.” Nature 527(7576): 105–9.

Faridounnia, Maryam, Gert E. Folkers, and Rolf Boelens. 2018. “Function and Interactions of ERCC1-XPF in DNA Damage Response.” Molecules 23(12): 1–25.

Gkirtzimanaki, Katerina et al. 2018. “IFNα Impairs Autophagic Degradation of MtDNA Promoting Autoreactivity of SLE Monocytes in a STING-Dependent Fashion.” Cell Reports 25(4): 921-933.e5. https://doi.org/10.1016/j.celrep.2018.09.001.

Glowicz. 2017. “乳鼠心肌提取 HHS Public Access.” Physiology & behavior 176(5): 139–48.

Glück, Selene et al. 2017. “Designed Experiments and Analysed the Data.” Nat Cell Biol 19(9): 1061–70. http://www.nature.com/authors/editorial_policies/license.html#terms.

González, Hugo, Daniela Elgueta, Andro Montoya, and Rodrigo Pacheco. 2014. “Neuroimmune Regulation of Microglial Activity Involved in Neuroinflammation and Neurodegenerative Diseases.” Journal of Neuroimmunology 274(1–2): 1–13. http://dx.doi.org/10.1016/j.jneuroim.2014.07.012.

Gordon, Siamon, and Philip R. Taylor. 2005. “Monocyte and Macrophage Heterogeneity.” Nature Reviews Immunology 5(12): 953–64.

Gurunathan, Sangiliyandi et al. 2019. “Review of the Isolation, Characterization, Biological Function, and Multifarious Therapeutic Approaches of Exosomes.” Cells 8(4): 307.

Harper, J. Wade, and Stephen J. Elledge. 2007. “The DNA Damage Response: Ten Years After.” Molecular Cell 28(5): 739–45.

Helena, Jolene Michelle et al. 2018. “Deoxyribonucleic Acid Damage and Repair: Capitalizing on Our Understanding of the Mechanisms of Maintaining Genomic Integrity for Therapeutic Purposes.” International Journal of Molecular Sciences 19(4).

Hervas-Stubbs, Sandra et al. 2011. “Direct Effects of Type I Interferons on Cells of the Immune System.” Clinical Cancer Research 17(9): 2619–27.

Hessvik, Nina Pettersen et al. 2016. “PIKfyve Inhibition Increases Exosome Release and Induces Secretory Autophagy.” Cellular and Molecular Life Sciences 73(24): 4717–37.

Hickey, William F., and Hiromitsu Kimura. 1988. “Perivascular Microglial Cells of the CNS Are Bone Marrow-Derived and Present Antigen in Vivo.” Science 239(4837): 290–92.

Holtman, Inge R. et al. 2015. “Induction of a Common Microglia Gene Expression Signature by Aging and Neurodegenerative Conditions: A Co-Expression Meta-Analysis.” Acta neuropathologica communications 3: 31. ???

Ioannidou, Anna, Evi Goulielmaki, and George A. Garinis. 2016. “DNA Damage: From Chronic Inflammation to Age-Related Deterioration.” Frontiers in Genetics 7(OCT): 1–8.

Jaarsma, Dick, Ingrid van der Pluijm, Gijsbertus T.J. van der Horst, and Jan H.J. Hoeijmakers. 2013. “Cockayne Syndrome Pathogenesis: Lessons from Mouse Models.” Mechanisms of Ageing and Development 134(5–6): 180–95. http://dx.doi.org/10.1016/j.mad.2013.04.003.

Jaspers, Nicolaas G.J. et al. 2007. “First Reported Patient with Human ERCC1 Deficiency Has Cerebro-Oculo-Facio- Skeletal Syndrome with a Mild Defect in Nucleotide Excision Repair and Severe Developmental Failure.” American Journal of Human Genetics 80(3): 457–66.

Kamileri, Irene, Ismene Karakasilioti, and George A. Garinis. 2012. “Nucleotide Excision Repair: New Tricks with Old Bricks.” Trends in Genetics 28(11): 566–73. http://dx.doi.org/10.1016/j.tig.2012.06.004.

Kaminskyy, V., and B. Zhivotovsky. 2010. “To Kill or Be Killed: How Viruses Interact with the Cell Death Machinery: Symposium.” Journal of Internal Medicine 267(5): 473–82.

Karakasilioti, Ismene et al. 2014. “Leading to Fat Depletion in NER Progeria.” 18(3): 403–15.

Lan, Yuk Yuen et al. 2019. “Extranuclear DNA Accumulates in Aged Cells and Contributes to Senescence and Inflammation.” Aging Cell 18(2): 1–12.

Lan, Yuk Yuen et al. 2014. “Dnase2a Deficiency Uncovers Lysosomal Clearance of Damaged Nuclear DNA via Autophagy.” Cell Reports 9(1): 180–92.

Leidal, Andrew M., and Jayanta Debnath. 2015. “Autophagy Devours the Nuclear Lamina to Thwart Oncogenic Stress.” Developmental Cell 35(5): 529–30. http://dx.doi.org/10.1016/j.devcel.2015.11.016.

Li, Tuo, and Zhijian J. Chen. 2018. “The CGAS-CGAMP-STI NG Pathway Connects DNA Damage to Inflammation, Senescence, and Cancer.” Journal of Experimental Medicine 215(5): 1287–99.

Liu, Siqi et al. 2015. “Phosphorylation of Innate Immune Adaptor Proteins MAVS, STING, and TRIF Induces IRF3 Activation.” Science 347(6227).

Lourbopoulos, Athanasios, Ali Ertürk, and Farida Hellal. 2015. “Microglia in Action: How Aging and Injury Can Change the Brain’s Guardians.” Frontiers in Cellular Neuroscience 9(FEB): 1–8.

Luo, Majing et al. 2016. “Nuclear Autophagy: An Evolutionarily Conserved Mechanism of Nuclear Degradation in the Cytoplasm.” Autophagy 12(11): 1973–83. http://dx.doi.org/10.1080/15548627.2016.1217381.

Madabhushi, Ram, Ling Pan, and Li Huei Tsai. 2014. “DNA Damage and Its Links to Neurodegeneration.” Neuron 83(2): 266–82.

Manuscript, Author. 2012. “Repair Endonuclease.” 10(7): 781–91.

Marteijn, Jurgen A., Hannes Lans, Wim Vermeulen, and Jan H.J. Hoeijmakers. 2014. “Understanding Nucleotide Excision Repair and Its Roles in Cancer and Ageing.” Nature Reviews Molecular Cell Biology 15(7): 465–81. http://dx.doi.org/10.1038/nrm3822.

Mathieu, Mathilde, Lorena Martin-Jaular, Grégory Lavieu, and Clotilde Théry. 2019. “Specificities of Secretion and Uptake of Exosomes and Other Extracellular Vesicles for Cell-to-Cell Communication.” Nature Cell Biology 21(1): 9–17. http://dx.doi.org/10.1038/s41556-018-0250-9.

Miranda, André M. et al. 2018. “Neuronal Lysosomal Dysfunction Releases Exosomes Harboring APP C-Terminal Fragments and Unique Lipid Signatures.” Nature Communications 9(1).

Morita, Rihito et al. 2010. “Molecular Mechanisms of the Whole DNA Repair System: A Comparison of Bacterial and Eukaryotic Systems.” Journal of Nucleic Acids 2010(ii).

Nakad, Rania, and Björn Schumacher. 2016. “DNA Damage Response and Immune Defense: Links and Mechanisms.” Frontiers in Genetics 7(AUG): 1–10.

Niedernhofer, L. J. et al. 2004. “The Structure-Specific Endonuclease Ercc1-Xpf Is Required To Resolve DNA Interstrand Cross-Link-Induced Double-Strand Breaks.” Molecular and Cellular Biology 24(13): 5776–87.

Niedernhofer, Laura J. et al. 2006. “A New Progeroid Syndrome Reveals That Genotoxic Stress Suppresses the Somatotroph Axis.” Nature 444(7122): 1038–43.

Niraula, Anzela, John F. Sheridan, and Jonathan P. Godbout. 2017. “Microglia Priming with Aging and Stress.” Neuropsychopharmacology 42(1): 318–33. http://dx.doi.org/10.1038/npp.2016.185.

Papandreou, Margarita Elena, and Nektarios Tavernarakis. 2019. “Nucleophagy: From Homeostasis to Disease.” Cell Death and Differentiation 26(4): 630–39.

Paul, Sophie et al. 2007. “Type I Interferon Response in the Central Nervous System.” Biochimie 89(6–7): 770–78.

Perry, V. Hugh, and Jessica Teeling. 2013. “Microglia and Macrophages of the Central Nervous System: The Contribution of Microglia Priming and Systemic Inflammation to Chronic Neurodegeneration.” Seminars in Immunopathology 35(5): 601–12.

Pogue, Sarah L. et al. 2004. “The Receptor for Type I IFNs Is Highly Expressed on Peripheral Blood B Cells and Monocytes and Mediates a Distinct Profile of Differentiation and Activation of These Cells.” Journal of Interferon and Cytokine Research 24(2): 131–39.

Raj, Divya D.A. et al. 2014. “Priming of Microglia in a DNA-Repair Deficient Model of Accelerated Aging.” Neurobiology of Aging 35(9): 2147–60. http://dx.doi.org/10.1016/j.neurobiolaging.2014.03.025.

Rello-varona, Santiago et al. 2016. “Autophagic Removal of Micronuclei Autophagic Removal of Micronuclei © 2012 Landes Bioscience . Do Not Distribute .” 4101(August): 170–76.

Rivest, Serge. 2009. “Regulation of Innate Immune Responses in the Brain.” Nature Reviews Immunology 9(6): 429–39. http://dx.doi.org/10.1038/nri2565.

Rothblum-Oviatt, Cynthia et al. 2016. “Ataxia Telangiectasia Orphanet Journal of Rare Diseases.” Orphanet Journal of Rare Diseases 11(159): 1–21. https://com-mendeley-prod-publicsharing-pdfstore.s3.eu-west-1.amazonaws.com/af98-PUBMED/10.1186/s13023-016-0543-7/13023_2016_Article_543_pdf.pdf?X-Amz-Security-Token=FQoGZXIvYXdzEIL%2F%2F%2F%2F%2F%2F%2F%2F%2F%2FwEaDOrC6aOVSnFDIak34iKfBOajRkA3P45L%2BRS6%2B.

Sarlus, Heela, and Michael T Heneka. 2017. “Microglia in Alzheimer ’ s Disease Find the Latest Version : Microglia in Alzheimer ’ s Disease.” Journal of Clinical Investigation 127(9): 3240–49.

Schumacher, Björn, George A. Garinis, and Jan H J Hoeijmakers. 2008. “Age to Survive: DNA Damage and Aging.” Trends in Genetics 24(2): 77–85.

Sedgwick, J. D. et al. 1991. “Isolation and Direct Characterization of Resident Microglial Cells from the Normal and Inflamed Central Nervous System.” Proceedings of the National Academy of Sciences of the United States of America 88(16): 7438–42.

Slawson, D. 1999. “How Effective Is Oral Nalmefene in the Treatment of Alcohol Dependence?” Evidence-Based Practice 2(11): 6, insert 2p. http://ezproxy.stir.ac.uk/login?url=http://search.ebscohost.com/login.aspx?direct=true&db=c8h&AN=2002080306&site=ehost-live.

Sok, Sophia P.M., Daisuke Ori, Noor Hasima Nagoor, and Taro Kawai. 2018. “Sensing Self and Non-Self Dna by Innate Immune Receptors and Their Signaling Pathways.” Critical Reviews in Immunology 38(4): 279–301.

Stemcell. 2015. “Neurological Disease Modeling.” 7(7): 1180–89. http://www.stemcell.com/en/Pages/Modeling-Human-Neurological-Disease-with-Induced-Pluripotent-Stem-Cells.aspx.

Stowell, Rianne D. et al. 2018. “Cerebellar Microglia Are Dynamically Unique and Survey Purkinje Neurons in Vivo.” Developmental Neurobiology 78(6): 627–44.

Stratigi, Kalliopi, Ourania Chatzidoukaki, and George A. Garinis. 2017. “DNA Damage-Induced Inflammation and Nuclear Architecture.” Mechanisms of Ageing and Development 165: 17–26. http://dx.doi.org/10.1016/j.mad.2016.09.008.

Sulli, Gabriele, Raffaella Di Micco, and Fabrizio D Adda Di Fagagna. 2012. “Crosstalk between Chromatin State and DNA Damage Response in Cellular Senescence and Cancer.” Nature Reviews Cancer 12(10): 709–20. http://dx.doi.org/10.1038/nrc3344.

Tang, D et al. 2013. “PAMPs and DAMPs: Signals 0s Taht Spur Autophagy and Inmunity.” Immunol Rev 249(1): 158–75.

Usselman, Charlotte W. Nina S. Stachenfeld Jeffrey R. Bender. 2017. “乳鼠心肌提取 HHS Public Access.” Physiology & behavior 176(3): 139–48.

Vaezi, Alec, Chelsea H. Feldman, and Laura J. Niedernhofer. 2011. “ERCC1 and XRCC1 as Biomarkers for Lung and Head and Neck Cancer.” Pharmacogenomics and Personalized Medicine 4(1): 47–63.

Wyss-Coray, Tony. 2016. “Ageing, Neurodegeneration and Brain Rejuvenation.” Nature 539(7628): 180–86.

Xu, Jing, Robert Camfield, and Sharon M. Gorski. 2018. “The Interplay between Exosomes and Autophagy - Partners in Crime.” Journal of Cell Science 131(15): 1–11.

Zhang, Conggang et al. 2019. “Structural Basis of STING Binding with and Phosphorylation by TBK1.” Nature. http://dx.doi.org/10.1038/s41586-019-1000-2.

Zhao, Xiao-Feng et al. 2019. “Targeting Microglia Using Cx3cr1-Cre Lines: Revisiting the Specificity.” Eneuro 6(4): ENEURO.0114-19.2019.

Zhu, Jiangao, Xiaopei Huang, and Yiping Yang. 2007. “Type I IFN Signaling on Both B and CD4 T Cells Is Required for Protective Antibody Response to Adenovirus.” The Journal of Immunology 178(6): 3505–10.

Acknowledgments

First and foremost, I want to express my gratitude to my supervisors Professor George Garinis and Post-Doctoral researcher Katerina Gkirtzimanaki for the support, encouragement and valuable feedback on my work.

Also, I am very thankful to the members of our laboratory (Katrakili Kavadina, Chatzinikolaou Georgia, Stratigi Callina, Goulielmaki Evi, Chatzidoukaki Ourania, Tsekrekou Maria, Batsiotos Nikolaos, Poutakidou Ioanna, Tsakani Edisona, Niotis Giorgos and Rouska Iliana), for the friendly attitude and support.

More personally, I would like to extend my appreciation to my family and my friends, who stood constantly by me this year in their unique way and for their patience.